

**COMPARISON OF A CYCLIC STEAM STIMULATION
ANALYTICAL MODEL USING "PSEUDO-PERMEABILITY"
WITH THE CONVENTIONAL APPROACH**



MOHD. HABIBUR RAHMAN



**DEPARTMENT OF PETROLEUM AND MINERAL RESOURCES ENGINEERING
BUET, DHAKA
BANGLADESH**

RECOMMENDATION OF THE BOARD OF EXAMINERS

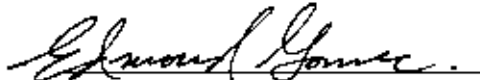
The undersigned certify that they have read and recommend to the Department of Petroleum and Mineral Resources Engineering, for acceptance, a thesis entitled COMPARISON OF A CYCLIC STEAM STIMULATION ANALYTICAL MODEL USING "PSEUDO-PERMEABILITY" WITH THE CONVENTIONAL APPROACH submitted by MOHD. HABIBUR RAHMAN in partial fulfillment of the requirements for the degree of MASTER OF SCIENCE in PETROLEUM ENGINEERING.

Chairman (Supervisor) :



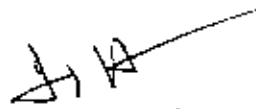
Dr. Mohammad Tanim
Head
Dept. of Petroleum & Mineral Resources Eng.
BUET

Member :



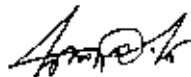
Dr. Edmond Gomes
Associate Professor
Dept. of Petroleum & Mineral Resources Eng.
BUET

Member :



Dr. Ijaz Hossain
Associate Professor
Dept. of Chemical Eng.
BUET

Member (External) :



Dr. Muhammad Mahbubul Alam
Associate Professor
Dept. of Mechanical Eng.
BUET

Date : January 20, 1998

ABSTRACT

Cyclic Steam Stimulation (CSS) process is a proven commercial oil recovery process in heavy oil reservoirs. CSS is mostly applicable for the reservoirs containing medium to high viscosity oil. In many of the heavier reservoirs, steam is injected under high pressure to create fractures (shear failure) in the reservoir. The changes in mass and heat transport properties created by steam invasion in the heterogeneously deformed shear failure zone have been shown to be the important factors for recovery mechanism. This work presents a new mathematical model, which considers the shear failure zone permeability in reservoir simulation by means of pseudo-relative permeability functions.

Fractures and microchannels are created in the shear failure zone of the reservoir during steam injection period. It is assumed that these fractures and microchannels remain during production period. As a result the reservoir permeability is altered from the original value. In this new model the actual permeability is calculated by using of pseudo-relative permeability functions.

The entire shear failure zone is divided into two concentric elliptical cylinders. The inner and outer cylinder is called hot and warm zone respectively. The flow rate is calculated from the well located at the center of an elliptical reservoir geometry.

The simulated results are obtained from this new model showing an excellent match with previously reported result in Cold Lake oil sands. The various production performance parameters (OSR, CDOR, WOR) as well as oil and water productions are calculated in eight cycles of operation. An extensive sensitivity study has been done for different physical and reservoir parameters. This model can be successfully used for simulating moderate to heavy oil reservoirs.

ACKNOWLEDGMENTS

I would like to express my sincere gratitude to Dr. Mohammad Tamim for his supervision and guidance throughout this thesis work. His encouragement, valuable advice made this work easy and successful.

I would like to thank Dr. Edmond Gomes, Associate Professor, Department of Petroleum and Mineral Resources Engineering, for his valuable suggestions and comments.

I would also like to express my gratitude to Dr. Ijaz Hossain, former Head of the Department of Petroleum and Mineral Resources Engineering for his encouragement to complete this work.

I appreciate the help of Mr. Zulfiquar Ali Reza, Lecturer, Department of Petroleum and Mineral Resources Engineering, in the computer implementation of the program.

TABLE OF CONTENTS

	Page
Abstract	i
Acknowledgments	ii
Table of contents	iii
List of Tables	v
List of Figures	v
Nomenclature	vii
Chapter I : Introduction	1
Chapter II : Review of the Literature	3
2.1 Analytical Model	4
2.2 Shear Failure	6
2.3 Elliptical Flow into a Well	8
2.4 Pseudo-Relative Permeability	10
2.4.1 Hysteresis of the Pseudo-Relative permeability	11
Chapter III : Model Development	14
3.1 The Flow Equations	15
3.1.1 Flow from Inner Hot Zone	15
3.1.2 Flow from Outer Warm Zone	15
3.2 Calculation of Pressure	17
3.3 Calculation of Temperature	18
3.3.1 Calculation of Initial Temperature	18
3.3.2 Calculation of Soak Temperature	19
3.3.3 Calculation of Production Temperature	20
3.4 Heat Loss Equation	20
3.5 Calculation of Saturation	21
3.6 Calculation of Viscosity	23
3.7 Calculation of Relative Permeabilities	24
Chapter IV : Computer Implementation	29

4.1	Model Description	29
4.2	Subroutines Used by Main Program	30
4.2.1	Initialization of the Program	30
4.2.2	Injection Period	32
4.2.3	Soak Period	33
4.2.4	Production Period	33
Chapter V :	Results and Discussion	35
5.1	Simulation Data	35
5.2	Elliptical Flow into a Well	38
5.3	Sensitivity Study	44
5.3.1	Effects of Soak Time	45
5.3.2	Effects of Steam Injection rates	48
5.3.3	Effects of Time Step Size	53
5.3.4	Effects of Steam Temperatures	53
5.3.5	Effects of Steam Quality	56
5.3.6	Effects of Formation Thickness	59
Chapter VI :	Conclusions and Recommendations	66
References	68
Appendix A :	Flow into a Well Located at the Center of an Elliptical drainage Boundary	75
Appendix B :	Calculation of Zone Temperature during Soak and Production period	84
Appendix C :	Calculation of Heat Loss to the Cap and Base Rock	87
Appendix D :	Calculation of Average Zone Saturation	90
Appendix E :	Calculation of Pseudo-Relative Permeabilities	92
Appendix F :	Calculation of Fluid Properties	94

LIST OF TABLES

	page
Table 5.1	Simulation input data 36
Table 5.2	Water-oil relative permeability 37
Table 5.3	Operational data 37

LIST OF FIGURES

Figure 3.1	Conceptual diagram of fluid and heat flow for the proposed model 16
Figure 3.2	Pressure dependent multiplication factor to relative permeability to water and oil 26
Figure 3.3	Relationship between degree of failure and reservoir pressure during production period 28
Figure 4.1	Computational flow diagram of the model 31
Figure 5.1	Comparison of cycle oil production 39
Figure 5.2	Comparison of cycle water production 39
Figure 5.3	Comparison of cumulative oil production 41
Figure 5.4	Comparison of cumulative water production 41
Figure 5.5	Comparison of cycle oil-steam ratio 42
Figure 5.6	Comparison of cycle water-oil ratio 42
Figure 5.7	Comparison of cycle calendar day oil production rate 43
Figure 5.8	Cycle oil production for different soak periods 46
Figure 5.9	Cumulative oil production for different soak periods 46
Figure 5.10	Cycle water production for different soak periods 47
Figure 5.11	Cumulative water production for different soak periods 47

Figure 5.12	Cycle oil production for various steam injection rates	49
Figure 5.13	Cumulative oil production for various steam injection rates	49
Figure 5.14	Cycle water production for various steam injection rates	50
Figure 5.15	Cumulative water production for various steam injection rates	50
Figure 5.16	Cycle oil-steam ratio for various steam injection rates	51
Figure 5.17	Cycle calendar day oil production rate for various steam injection rates	51
Figure 5.18	Cycle water-oil ratio for various steam injection rates	52
Figure 5.19	Cycle oil production for various time step sizes	54
Figure 5.20	Cumulative oil production for various time step sizes	54
Figure 5.21	Cycle water production for various time step sizes	55
Figure 5.22	Cumulative water production for various time step sizes	55
Figure 5.23	Cycle oil production for different steam temperature	57
Figure 5.24	Cumulative oil production for different steam temperature	57
Figure 5.25	Cycle water production for different steam temperature	58
Figure 5.26	Cumulative water production for different steam temperature	58
Figure 5.27	Cycle oil production for various steam qualities	60
Figure 5.28	Cumulative oil production for various steam qualities	60
Figure 5.29	Cycle water production for various steam qualities	61
Figure 5.30	Cumulative water production for various steam qualities	61
Figure 5.31	Cycle oil production for different pay thickness	62
Figure 5.32	Cumulative oil production for different pay thickness	62
Figure 5.33	Cycle water production for different pay thickness	63
Figure 5.34	Cumulative water production for different pay thickness	63
Figure 5.35	Cycle oil-steam ratio for various pay thickness	64
Figure 5.36	Calendar day oil production rate for various pay thickness	64

NOMENCLATURE

a	= major axis of the ellipse (m)
A	= area (m^2)
b	= width of fracture (m), minor axis of the ellipse (m)
c	= compressibility (kPa^{-1}), half length of the line source (m)
C	= specific heat ($\text{kJ m}^{-3}\text{K}^{-1}$), fluid loss coefficient ($\text{m d}^{-1/2}$)
d	= diffusivity length (m)
E_c	= energy stored in the cap and base rock (kJ)
f	= degree of failure (fraction)
g	= acceleration due to gravity (9.81 ms^{-2})
h	= formation thickness (m), specific enthalpy (kJ kg^{-1})
h_{fg}	= latent heat of vaporization (kJ kg^{-1})
H	= dimensionless heat input
i	= steam injection rate ($\text{m}^3 \text{ day}^{-1}$)
k	= absolute permeability (m^2)
k_h	= thermal conductivity ($\text{kJ m}^{-1} \text{ d}^{-1} \text{ K}^{-1}$)
k_{ro}^*	= pseudo relative permeability of oil (fraction)
k_{rw}^*	= pseudo relative permeability of water (fraction)
K	= hydraulic conductivity (ms^{-1})
K_{md}	= number of total cycles
L	= distance (m)
L_f	= fracture half length (m)
L_v	= latent heat of vaporization (kJ kg^{-1})
M	= mobility ratio, volumetric heat capacity (kJ kg^{-1})
p	= pressure (kPa)
p_{sat}	= saturation pressure (kPa)
q	= fluid flow rate ($\text{m}^3 \text{ day}^{-1}$)
q_L	= heat loss rate (kJ s^{-1})

Q	= heat flow rate (kJ day^{-1})
r	= radius (m)
R	= radius in polar coordinates
S_{wi}	= irreducible water saturation (fraction)
S_o	= oil saturation (fraction)
S_{or}	= residual oil saturation (fraction)
S_p	= spurt loss quotient
S_w	= initial water saturation (fraction)
S_{wr}	= residual water saturation (fraction)
t	= time (day)
T	= temperature
\bar{T}	= $(T - T_r)/(T_s - T_r)$
U	= unit step function
v	= variable of integration
V	= volume (m^3)
V_f	= fluid leak-off velocity ($\text{m}^3 \text{s}^{-1}$)
x_i	= steam quality
X_o	= relative permeability multiplication factor for oil
X_w	= relative permeability multiplication factor for water

Greek Symbols

α	= thermal diffusivity ($\text{m}^2 \text{s}^{-1}$), effective fracture width (m)
β	= 1, thermal expansion coefficient (K^{-1})
λ	= mobility ($\text{m}^2 \text{Pa}^{-1} \text{s}^{-1}$)
δ	= fluid heat loss due to production (fraction)
ε	= eccentricity of the ellipse (fraction)

Φ	= potential function
ϕ	= porosity (fraction)
Γ	= dimensionless x coordinate
η	= dimensionless z coordinate, hydraulic diffusivity
μ	= dynamic viscosity (Pa.s)
ξ	= dimensionless y coordinate
ρ	= density (kg m^{-3})
τ	= dimensionless time
τ_f	= dimensionless time for steam advancement in the fracture
τ_{sa}	= dimensionless time for the steam to move into the formation
θ	= dimensionless temperature, angle
ν	= kinematic viscosity ($\text{m}^2 \text{s}^{-1}$)
π	= pi = 3.14159265

Subscripts

0	= interface between reservoir and the adjacent strata
1	= hot
2	= warm
b	= bulk, interface
c	= condensate
d	= drainage
e	= external
f	= formation, fluid
h	= hot, interface
i	= initial, injected
o	= oil
om	= mobile oil
p	= pore

r	= radial
R	= reservoir
s	= steam
sa	= steam advance
sc	= standard condition
st	= stock tank, steam
t	= total
w	= water, wellbore, warm
wc	= connate water
wf	= flowing wellbore
wm	= mobile water
z	= vertical co-ordinate

Abbreviations

CDOR	= calendar day oil rate
CSS	= cyclic steam stimulation
CWE	= cold water equivalent
EFW	= elliptic flow into a well
OSR	= oil-steam ratio
PDOR	= production day oil rate
WOR	= water-oil ratio

Chapter I
INTRODUCTION



Thermal methods of enhanced oil recovery (EOR) are very effective for reservoirs which contain medium to high viscosity oil. Basically, two classes of thermal recovery processes are used widely : displacement or drive processes and stimulation processes. Cyclic Steam Stimulation (CSS) process is one of the most important stimulation processes for enhanced oil recovery methods. Steam stimulation involves periodic injection of steam into a producing well for several days to a few weeks. Then the well is allowed a soaking period to dissipate energy and form a heated zone in the vicinity of the wellbore. The hot oil and water are then produced from the heated zone after soaking period.

Steam was first used for recovering heavy oil in Woodson, Texas in 1931. CSS has received intense interest by the heavy oil producers since the early 1960s. Steam stimulation is the most recognized process for recovering heavy oil. It is being used successfully all over the world: California, Alberta and Venezuela.

Cyclic Steam Stimulation is a very difficult process to history match using thermal simulators. The main reason is the fact that the reservoir undergoes many changes in pressure, temperature and saturations as well as permeability. The creation of fractures and microchannels in the shear failure zone during injection period makes the process even more complex. Although numerous steam injection operations have been carried out, many of the complexities of the operation are still unknown. It is difficult to develop a unique solution procedure for CSS. Numerical simulator has made rapid progress with the advance of computing power. Difficult problems are now investigated by simulators. On the other hand they are very expensive and time consuming ventures. Good analytical solution is still a very useful tool.

In literature, a number of analytical models have been proposed but few of them have considered shear failure phenomena. Arthur et al.(1991) and Tamim and Farouq Ali (1995) considered the fracturing phenomena during injection period in CSS process which often occurs in heavy oil sands. Both the models considered elliptical flow geometry with an open fracture at the wellbore whereas Tamim et al. also investigated the closed fracture situation. None of them considered shear failure. Most of the simulators do not include the geomechanical aspect of the CSS process.

A new analytical model for Cyclic Steam Stimulation of heavy oil reservoirs that includes the fractures and microchannels in the shear failure zone, saturation changes and pressure dependent relative permeability has been proposed. The model considers the fractures and microchannels in the shear failure zone to remain open or partially open during production period. The enhanced permeability in the shear failure zone has been calculated by using pseudo-relative permeability functions. An elliptical flow geometry of the entire failure zone have been considered for simulation purpose. The model has been validated by comparing results with available field data.

REVIEW OF THE LITERATURE

Cyclic Steam Stimulation(CSS) is most widely used thermal method for heavy oil recovery. High pressure steam increases the mobility of oil and by creating a shear failure zone, it also increases the permeability of the producing zone. Due to the heterogeneous nature of the reservoir, it is difficult to correlate all reservoir parameters regarding the production performance. The extent and orientation of fractures in the shear failure zone affect the productivity of the process. The productivity of the oil also depends on the drive and drainage mechanism. The natural drive mechanisms are: gravity drainage, formation compaction, fluid expansion and solution gas drive. Gravity drainage is an important drive mechanism in CSS process.

The viscosity of the oil and permeability of the reservoir are two important parameters that dominate the flow rate during production period. The actual permeability is altered in the reservoir due to the creation of fractures and microchannels in the shear failure zone during steam injection process. The extent of failure zone and temperature distributions have significant importance in reservoir simulation. The relative permeability of the reservoir in a water/oil system also depends on the reservoir temperature. Because relative permeability to oil increases and to water decreases as temperature increases (Nakamthap, 1986). The viscosity reduction and permeability enhancement are the main purpose of cyclic steam stimulation process.

There are three types of cyclic steam stimulation modeling approaches: (1) empirical correlations, (2) multicomponent multiphase thermal simulators and (3) analytical models (Sylvester and Chen, 1988). Empirical correlations can be used for correlating data. They have limiting predictive utility. Thermal simulators yield rigorous solutions to the material and energy balance, but it is not suitable for a quick analysis of steam

injection projects. It is much more expensive and time consuming and as well as more sensitive to rock and fluid property data. Analytical models can account for many of the important physical phenomena and is capable of providing quick and reasonably accurate predictions of field performance.

2.1 Analytical Models

CSS analytical models meet the need for quickly predicting field performance. Several analytical models have been developed. Some of the main models found in the literature are reviewed here.

Boberg and Lantz (1966) presented a simplified analytical model for calculating multicycle steam stimulation behavior. They used the Marx-Langenheim equation to calculate the initial radius of the reservoir heated to steam temperature during the injection phase of the process. They also accounted for heat loss through conduction both vertically and radially. They assumed that the reservoir is uniformly heated to a calculated distance from the wellbore. The size of the heated region is determined by accounting for heat losses to the over and underburden. This model successfully matched the production history of a number of steam stimulated wells such as Quiriquire Well. It is most accurate for the first cycle of stimulation and becomes progressively less accurate for the succeeding cycles; because of the simplifying assumptions made. The major limitation of this model is that it is not applicable to thick sands. Where the gravity segregation of steam and oil will result highly non uniform heating of the oil around the wellbore.

Gontijo and Aziz (1984) presented a simple analytical model for simulating heavy oil recovery by cyclic steam stimulation in pressure-depleted reservoirs. They described that the flow rate of oil is influenced by oil viscosity, effective permeability of the heated zone, porosity, mobile oil saturation and thermal diffusivity of the reservoir. The

potential included the gravity term and a conical shaped steam zone was assumed. They concluded that the predicted response of the reservoir to steam injection by both the analytical and numerical models is similar.

Sylvester and Chen (1988) presented an improved cyclic steam stimulation model for predicting heavy oil recovery from pressure depleted reservoirs. They used a modified gravity drainage inflow equation to predict the production rates for both oil and water. The model permits the direct input of field data or correlation for relative permeability. They concluded that the model produced an excellent history match of oil production and water cut up to seven cycles.

Arthur, Best, Jha and Mourits (1991) presented an analytical composite model for cyclic steam stimulation in elliptical flow geometry. They considered the reservoir consisting of two distinct region of different fluid properties, porosity and permeability. They used the fluid flow and heat and mass balance equations for obtaining pressure, temperature and average phase saturation in the hot and cold zones. The effect of two phase oil and water flow in the reservoir was considered by using relative permeability. They reported good history match with both field data and numerical simulation results.

Tamim and Farouq Ali (1995) presented a new mathematical model, involving analytical techniques for Cyclic Steam Stimulation (CSS) performance prediction. In their model, a fracture heating computation coupled with fluid flow - both during injection and production was considered. This was based upon two criteria: a fracture flow and flow in an elliptical geometry with a circular well in the center. They assumed that a vertical fracture is created during steam injection. A comprehensive investigation was made for a completely closed fracture during production period. The results obtained from this investigation did not properly match with field data. They suggested existence of a partially open fracture during production period. The most significant achievement of this model was to developed a technique for calculating average viscosity, based on the actual areal distribution of temperature during production. No

stress analysis in the shear failure zone was done in this model. They reported that the model could serve as a valuable guideline for numerical simulation or physical modeling.

2.2 Shear Failure

During steam injection in heavy oil reservoirs, shear failure zone is created in the reservoir along the initial shear band due to high injection pressure of the steam. The steam injectivity and oil-water production rates depend on the size, shape and extent of the shear failure zone. The actual shape and the orientation of the failure zone was not completely understood. Some of the key papers about shear failure zone are reviewed here.

Ito (1984) proposed in his sand deformation model, horizontal fractures were created in the shear failure zone. When steam is injected into the formation under high pressure, a fracture is created and extends through the formation. The fracture orientation depends on the depth of the reservoir. Therefore, at shallow depths induced fractures are more likely to be horizontal or intersect a horizontal plane at a small angle. He postulated in his model a new flow geometry to achieve a realistic interpretation of well performances. The new flow geometry has been termed as the "sand deformation concept". He described in his sand deformation model the changes in porosity, pressure level and energy and flow characteristics resulting from the existence of microchannels. The injected fluid was able to penetrate in the unconsolidated oil sand by creating microchannels. He reported that the most important phenomenon for the recovery of bitumen was the one-way-valve effect of the microchannels that are created during the injection phase of CSS and are closed during the production phase. He concluded that, the new model provided an excellent match for all available observations like steam injection pressure, oil and water production rates, fluid production temperature and salinity changes of an actual well.

Settari (1989) described a new formulation of non-linear soil mechanics and multiphase thermal flow. The shear failure in the formation is caused by the non-linearities of the soil behavior and their interactions with fluid flow. He included in his model: a) nonlinear compressibility and flow properties as function of pressure, stress and temperature b) non-linear, incremental, thermal poroelastic stress analysis, and c) shear failure and its effect on transport properties, porosity and stress. The physics of the model accounts for nonlinear soil mechanics behavior, soil failure and their effect on porosity and permeability of the media. He showed that the formation failure is a function of thermal and poroelastic stresses. The nonlinearity of the compressibility and failure are the principal mechanisms controlling the injectivity in oil sands. Shear failure around an injector or at fracture face is an important mechanism which further increases mobility. He described that this effect confirmed and quantified the intuitive concepts of "sand deformation" or "microchannelling". He also described that for a sufficiently high injection pressure, failure will occur with an increase of permeability and porosity in the shear zone. He reported that the model was in good agreement with the injectivity and fracture dimensions of most of the oil-sands.

Teufel and Rhett (1991) described the geomechanical evidence of shear failure during production of the Ekofisk field. The shear failure occurred during the compaction of high porosity chalk as the shear stress increased with pressure drawdown. The shear failure during depletion increased fracture density and reduced the dimensions in the fractured reservoirs, thereby maintain initial reservoir permeability. They suggested that the shear failure process could account for the continued good producibility of the Ekofisk field, in spite of compaction.

Ito, Settari and Jha (1993) presented a numerical model considering the geotechnical aspects of tar sands. Based on the geomechanical findings, they described the shear failure zone will develop in several stages. First, shear bands are generated from the tensile fracture due to lowering of effective stresses adjacent to the fracture face. The alteration of the local stress field due to the widening of the fracture will also contribute

to the generation of the shear bands. The injected fluid has a tendency to leak-off into these shear bands. Second, this fluid encroachment causes pore pressure in the shear zone to increase sharply due to the high mobility of the injected fluid and generates a low minimum effective stress in the shear zone. They described this would enhance the propagation of the shear failure zone. In this stress zone, the injected fluid will not traveled evenly. It will flow in its own path, and resident fluid will occupy the remainder of the zone. As a result the dendritically connected flow paths from the injection well through fracture and shear planes are generated. They reported that this phenomena would increase the permeability in the shear failure zone. They showed that the changes in mass and heat transport properties are significant factors for the recovery mechanism. They described the theoretical and practical aspects of shear failure zone in reservoir simulation, by means of pseudo relative permeability functions. The pseudo-relative permeability functions were derived by considering the shear failure phenomena. They reported that the pseudo relative permeability model in shear failure zone for reservoir simulation gave better history match in production performance.

2.3 Elliptical Flow into a Well

During steam injection in CSS process, shear failure zone is created around the wellbore. The flow from failure zone into the well is known to be elliptic during production period (Tarnim and Farouq Ali, 1995). Some key papers about elliptic flow into the wellbore are reviewed here.

van der Ploeg, Kirkham and Boast (1971) presented an exact solution for steady saturated flow to a fully penetrating well in an elliptical confined aquifer. They considered the aquifer is isotropic and homogeneous. The potential and steam functions for a number of different shaped aquifers and well locations are developed by starting with a general solution to Laplace's equation. They concluded that the variety

of geometries enables one to predict the well discharge for aquifers which approach the shape of an ellipse. This means that the well may be located at different position of the elliptical aquifer.

Dietrich (1986) presented a Cyclic Steam Stimulation model of tar sands through hydraulically induced fracture. He assumed an elliptical heating pattern as hot injection fluid moved off a vertical fracture face. The heat retained in the reservoir, base and cap rock in an approximately ellipsoidal region. The isotherms were determined on the basis of temperature computed in the reservoir after multiple steam cycles in a vertically fractured well. He attributed the closure of fracture to expansion of rock, because of pore pressure build up and assumed that it closed slowly over a period of days. He concluded that the lengths of the major and minor axes of the heated ellipsoid were important, because they influenced the choice of well spacing and the time of interwell heat communication.

Arthur, Best, Jha and Mourits (1991) developed an analytical model for cyclic steam stimulation in reservoirs with elliptical flow geometry. They divided the entire flow geometry into a hot and a warm zone. The hot zone was bounded by the profile of the 100°C isotherm and the warm zone by an isotherm 1°C above the initial reservoir temperature. They assumed that the length of the fracture obtained during steam injection for a particular cycle does not change at the end of the production period for that cycle. They reported that the model provided a rapid evaluation of the performance of cyclic steam stimulation projects for the purpose of optimization and for process control of commercial operations.

Tanim and Farouq Ali (1995) presented an analytical cyclic steam stimulation model including formation parting. The model based upon a fracture heating computation, coupled with fluid flow - both during steam injection and oil and water production. In their model three different flow equations were considered: (1) flow into a wellbore at the center of an elliptical drainage boundary, (2) flow from a finite line source into a

well and (3) flow into a partially open fracture in an elliptical drainage area. They investigated a completely close fracture during production period. It failed to match the field performance results. On the basis of flow rates found in elliptical geometry with a circular well in the center, they suggested that a partially open fracture exist during production period. They did not consider the shear failure phenomena and enhanced permeability in the failure zone in their model. They concluded that the flow into a circular wellbore at the center of an elliptical flow geometry did not represent the flow pattern in the field, because it underestimated the production.

2.4 Pseudo-Relative Permeability

The CSS process is a proven, commercially well recognized recovery process in heavy oil reservoirs. So far, the actual recovery mechanism has not been completely understood. It is true that the shear failures are created in the heavy oil reservoirs during steam injection in cyclic steam stimulation process. Recently a few of the works have been done on the CSS process considering the geomechanical aspects of the reservoirs. The physical and fluid flow properties in the heterogeneously deformed failure zone have been shown to be the important factors for the recovery mechanism. The pseudo-relative permeability functions are used to represent the shear failure zone in numerical reservoir simulation.

The pseudo-relative permeability is defined as the altered relative permeability in the heterogeneously deformed shear failure zone of the reservoir (Ito et al., 1993). The pseudo-relative permeability is used for the purpose of reservoir simulation, where large permeability variation exist in the reservoirs during production period of the CSS process. Based on the above mentioned work, detailed description of the pseudo-relative permeability and its use are presented.

Sometimes pressure dependent relative permeability hysteresis is used in the reservoir simulation of steam stimulation process, but its mechanism is not clear. As steam is injected into a relatively incompressible reservoir, pore pressure increases and the effective stress decreases. At pore pressure corresponding to low effective stresses, the formation compressibility increases by about two order of magnitude, and shear failure occurs. This phenomenon result in dilation, with rapid increases in porosity and permeability (Ito et al.,1993). This enhanced permeability is calculated by using pseudo-relative permeability functions. The geomechanical aspect of shear failure has the following features (Ito et al.,1993).

1. High K_{rw} is expected in the areas where the pressure is higher than the pressure which would cause the sands to fail.
2. Since the shear failure is generally associated with the dilation of formation, a porosity change also appears along with the high K_{rw} zone.
3. Shear failure seems to take place along the initial shear band, therefore high K_{rw} should appear in only certain directions.

2.4.1 Hysteresis of the Pseudo Relative Permeability

Heterogeneous flow paths that were created during the injection period, remains unchanged during the early production period. When pore pressure is decreased due to the fluid production, the flow paths are closed partially or the connections between the paths start to break. The high relative permeability starts to decrease, and retain the residual value. The magnitude of the hysteresis depends on the physics of the remoulding process and also the reservoir pressure. During the stabilized production period, the shear planes may still exist and the residual porosity and permeability due to

failure during the injection period may also exist in the formation. The residual porosity and permeability are generally higher than the original value (Ito et al, 1993).

During the injection period, the injected fluid passes through the microchannels of shear planes in the failure zone. Thus water saturation in the failure zone is significantly higher than the surrounding reservoir. The water relative permeability in the failure zone is also much more higher than the surrounding reservoir. To accommodate this heterogeneity in the reservoir properties, the pseudo relative permeability is used.

Some of the key papers about pseudo relative permeability for reservoir simulation are reviewed here.

Hearn (1971) presented a method for developing pseudo-relative permeability curves in two dimensional simulation of fluid displacement projects, where vertical sweep is affected primarily by the variation of permeability. He used pseudo relative permeability functions in a mathematical model for calculating vertical efficiency using a stratified reservoir concept. Basic reservoir data was used to generate pseudo relative permeability curves that reflected the degree of vertical permeability variation. He concluded that the model was more applicable to water drive than to gas-injection projects where density differences may be large.

Jacks, smith and Mattax (1973) presented a method for the modeling of three dimensional reservoirs with two dimensional reservoir simulators using dynamic pseudo functions. They derived dynamic pseudo relative permeabilities from cross-sectional model and showed that the dynamic pseudo relative permeabilities are applicable over a wide range of rates and initial fluid saturations. They reported that the dynamic pseudo relative permeabilities were strongly dependent on initial reservoir saturations and flow velocity. They concluded that the correlation and techniques developed in their study, to account for saturation and velocity effects, should be applicable to other reservoir systems.

Ito, Settari and Jha (1993) presented a reservoir simulation model, where they considered the effects of shear failure on the cyclic steam stimulation process and pseudo functions. They described, in their paper, the theoretical and practical aspects of representing the shear failure zone in reservoir simulation by means of pseudo relative permeability functions. They reviewed the relative permeability hysteresis that is commonly used in the simulation of the steam stimulation process. A new set of stress-dependent pseudo relative permeability was proposed and also presented a practical method for the use of the pseudo functions in a reservoir simulator. The method could be applied to injection, as well as production cycles. The model was tested with the actual data from the Esso Cold Lake tar sand operation. They reported that the new model provided a better representation of the field performance than the conventional model.

Barker and Thibeau (1997) presented a critical review of the use of the pseudo relative permeabilities for upscaling. They summarized the properties and limitations of different dynamic pseudo relative permeability methods. They described some severe difficulties common to all methods such as choosing the number and locations of the coarse-grid rock types, defining the simulations from which the pseudo relative permeabilities are generated and the dependence of the pseudo relative permeabilities on well rates and positions. They reported that, in practice, pseudo relative permeabilities cannot be used reliably to scale up from a "fine-grid" geological model to a "coarse-grid" fluid flow model except for cases where capillary or gravity equilibrium can be assumed at the coarse-grid block scale. They concluded that scaling up from the core scale to the geological model is more likely to be possible because capillary forces are more important at smaller scales.

Chapter III

MODEL DEVELOPMENT

The importance of cyclic steam stimulation process is ever increasing for recovering heavy oil. Analytical models are well-known to make good predictions of this rather complex process. There are lots of paper published about CSS process. None of the analytical models consider elliptical flow into a unfractured wellbore. Shear failure zone is created around the wellbore during steam injection process in the heavy oil reservoirs. The fluid flow, heat transfer, mass balance, fluid saturations and relative permeability as well as the extent of shear failure zone are the important factors for developing the model. It is difficult to analyze all of the physical and reservoir parameters. The shear failure zone is complex in nature. It is generally associated with volumetric dilation or sand compaction, a porosity change and the flow paths are dendritically connected. Since the volumetric dilation or sand compaction is taken place in the shear failure zone. As a result the permeability and porosity of the shear failure zone are altered. A new analytical technique has been developed in this work which considers all of the physical and reservoir parameters.

The degree of failure, fluid saturations change, pressure dependent relative permeability and extension of shear failure zone are the key parameters that have been considered in this new model. An elliptical flow system have been considered from the shear failure zone into the wellbore during production period. Tamim and Farouq Ali (1995) considered in their analytical model the vertical fracture created during injection period remain partially open during production period. In this new model the permeability enhancement due to the existence of shear failure zone during production period is simulated by using pseudo-relative permeability functions.

3.1 The Flow Equations

The model is based on the elliptical flow geometry. The entire reservoir is divided into two concentric elliptical cylinder on the basis of isotherms. A conceptual diagram of the fluid and heat flow is shown in Figure 3.1. For convenience of analysis, inner zone is called the hot zone and the outer zone is called the warm zone.

3.1.1 Flow from Inner Hot Zone

It is assumed that the shear failure zone created during steam injection period also exists during the production period. It has been described in Chapter II, Section 2.3 that the drainage area in such reservoirs are elliptical shaped hot zones with a circular wellbore at the center. van der Ploeg, Kirkham and Boast (1971) Presented an exact solution for steady saturated elliptical flow into a fully penetrating well. The flow rate can be expressed by (detail in Appendix A),

$$q = \frac{-2\pi K h \Delta\Phi A_{NO}}{\ln\left(\frac{a}{r_w}\right)} \quad (3.1)$$

where K is the hydraulic conductivity of the reservoir, h is the reservoir thickness, $\Delta\Phi$ is the difference in hydraulic head, A_{NO} is the orthonormal functions coefficient, a is the major axis of the ellipse and r_w is the wellbore radius.

3.1.2 Flow from Outer Warm Zone

Muskat (1937) presented an equation for steady state flow case. The following equation accounts the flow rate from outer warm zone at each time step.

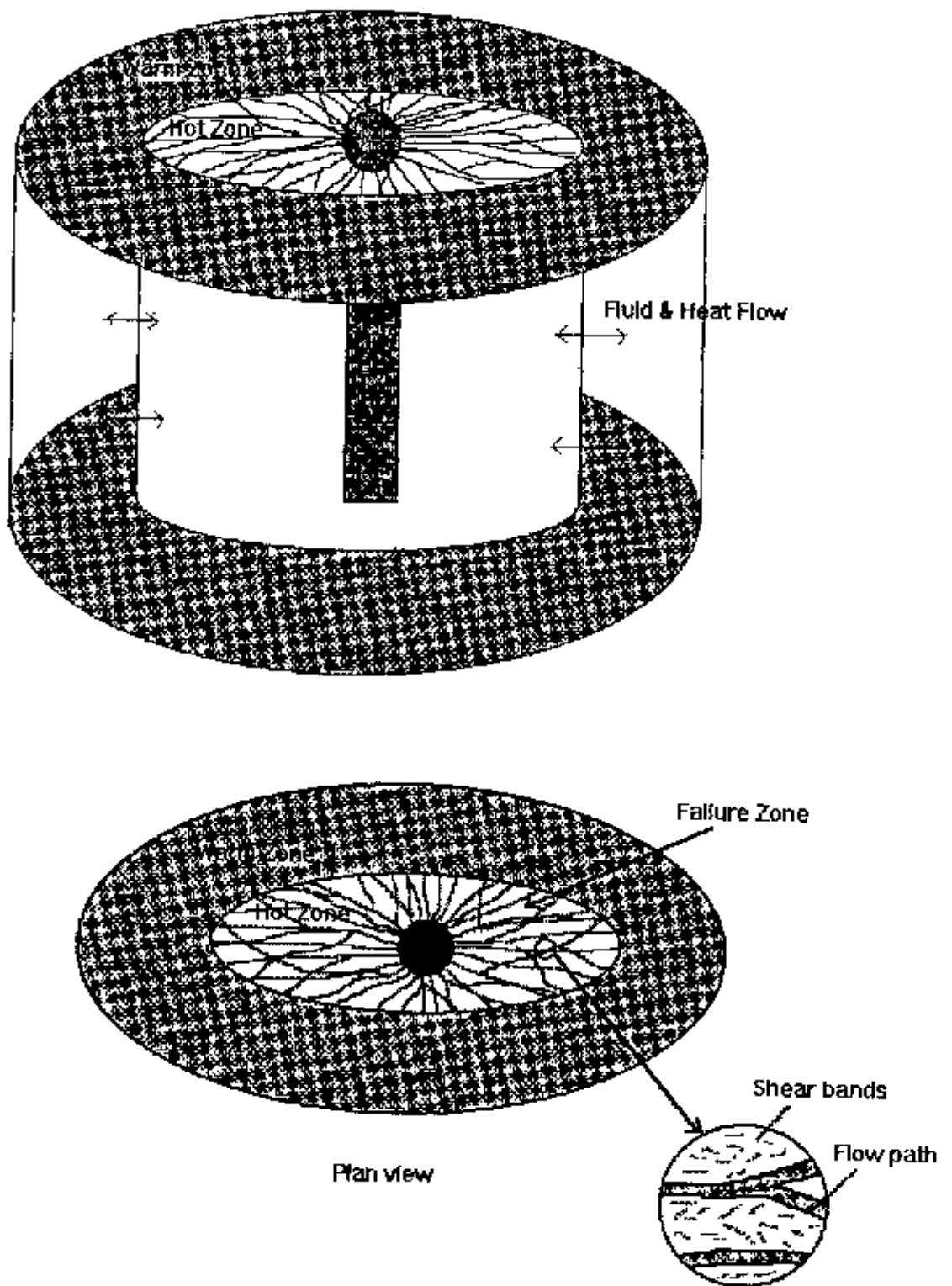


Figure 3.1 - Diagram of fluid flow and heat transfer for the proposed model.

$$q = \frac{2\pi k h (p_e - p_b)}{\mu \ln \left(\frac{a_e + b_e}{a_b + b_b} \right)} \quad (3.2)$$

3.2 Calculation of Pressure

The reservoir pressure is determined by calculating the average fluid height in the particular zone of the reservoir. Tamim and Farouq Ali (1995) developed the following material balance equations which are used for estimating the average fluid heights in this model. The average fluid heights at any time n for the hot and warm zones are

$$\bar{h}_{hot}^n = \bar{h}_{hot}^{n-1} - (Q_{hot} - Q_{warm}) / \phi A_{hot}, \quad (3.3)$$

$$\bar{h}_{warm}^n = \bar{h}_{warm}^{n-1} - Q_{warm} / \phi A_{warm}, \quad (3.4)$$

where Q is the total fluid flow at each time step.

The interface pressure of two zone is determined by calculating the interface fluid height. The area-weighted average method is used to determine the interface fluid height.

$$h_b = \frac{\bar{h}_{hot} A_{hot} + \bar{h}_{warm} A_{warm}}{A_{hot} + A_{warm}} \quad (3.5)$$

It is assumed that the outer drainage boundary pressure is to be the initial reservoir pressure.

3.3 Calculation of Temperature

The calculation of average reservoir temperatures in this new analytical model of cyclic steam stimulation process are divided into three categories. These are:

1. Initial temperature calculation
2. Average soak temperature calculation and
3. Production temperature calculation

3.3.1 Calculation of Initial Temperature

In cyclic steam stimulation process, steam is injected into the reservoir for increasing the mobility of the reservoir fluids. Wheeler (1969) proposed the following equation which gives the temperature profile at any point in the reservoir for the given injection rate and time

$$\bar{T}(\Gamma, \xi, \eta, \tau) = U(\tau - \tau_s) \frac{\xi}{\sqrt{\pi \sqrt{\tau - \tau_s}}} \int_0^1 \operatorname{erfc} \left\{ \frac{\sqrt{\beta} [v^2(\tau - \tau_s)] + \frac{\eta}{2\beta}}{\sqrt{\gamma(\tau - \tau_s)(1 - v^2)}} \right\} \times \exp \left\{ - \left[\frac{\xi}{2v\sqrt{\tau - \tau_s}} \alpha v \sqrt{\tau - \tau_s} \right]^2 \right\} \frac{dv}{v^2} \quad (3.6)$$

The steam front propagation time can be calculated by the following dimensionless time equation

$$\Gamma = 2H\sqrt{\tau_s} \int_0^1 \operatorname{erfc} \left[V^2 \sqrt{\frac{\beta\tau_s}{\alpha(1-v^2)}} \right] \operatorname{ierfc}(\alpha v\sqrt{\tau_s}) dv \quad (3.7)$$

The temperature in the shear failure zone follows by a step function profile. Initially only condensate flows in the formation. Once the energy supplied to the failure zone exceeds the energy transferred into the formation, a steam zone will advance. The steam advancing time is calculated by the following equation,

$$\frac{1}{\alpha\sqrt{\tau_{sa}}} \operatorname{ierfc}(\alpha\sqrt{\tau_{sa}}) = \frac{2x_f h_{fg}}{C_f(T_i - T_f)} \quad (3.8)$$

In the hot zone boundary, an isotherm of 100°C is used and in the warm zone boundary, an isotherm of 0.01 degree above the initial reservoir temperature is used. Average temperature of the two zones is estimated by using linear polynomial approximation.

3.3.2 Calculation of Average Soak Temperature

During soak period the temperatures in the hot and warm zones decline slightly from those at the end of injection due to heat losses to impermeable strata. Tamim and Farouq Ali (1995) developed the following overall heat balances to calculate the average zone temperatures during soak period. This heat balance equations are used in the present model.

Hot zone heat balance:

Heat content = over/underburden heat loss + warm zone heat loss

Warm zone heat balance:

Heat content = over/underburden heat loss - heat gain from hot zone.

3.3.3 Calculation of Average Production Temperature

After production starts, the hot and warm zone temperatures are decreased due to fluid production and heat losses to the impermeable strata. Arthur et al. (1991) assumed that the thermal and fluid properties are changed with temperature during production but are essentially constant for a small time step. The overall heat balance equations proposed by Tamim and Farouq Ali (1995) are used in this study for calculating average zone temperatures during production period.

Hot zone heat balance:

Heat content = production heat loss + over/underburden heat loss + warm zone heat loss - heat gain from warm zone flow.

Warm zone heat balance:

Heat content = heat loss to hot zone flow + over/underburden heat loss - heat gain from hot zone.

The details of the description for calculating zone temperature during soak and production period were presented in Appendix B.

3.4 The Heat Loss Equation

The heat loss to the over/underburden by conduction from reservoir in CSS process is common phenomena. Many authors suggested that, maximum heat was lost during soak period. Tamim and Farouq Ali (1995) used one-dimensional heat conduction equation for heat loss to the cap and base rock. Inserting the fitting function (Vinsome

and Westerveld, 1980) into the one dimensional heat conduction equation they found the following equation.

$$\frac{T_0 - T_0^N}{\Delta t} = \alpha_h \left(\frac{T_0}{d^2} - \frac{2p}{d} + 2q \right), \quad (3.9)$$

Where α_h is the thermal diffusivity, T_0 is the interface temperature, d is the diffusivity length and p and q are parameters. T_0^N is the interface temperature at the beginning of the time count. The following equations are used to calculate the heat loss rate and energy stored in the cap and base rock.

$$q_t = k_h \left(\frac{T_0}{d} - p \right) \quad (3.10)$$

$$E_c = \frac{k_h}{\alpha_h} d (T_0 + pd + 2qd^2) \quad (3.11)$$

where k_h is thermal conductivity. Details of the above equations were presented in the Appendix C.

3.5 Calculation of Saturation

Accurate calculation of fluid saturations is an important factor for any simulation process. The fluid saturation is changed due to the creation of fractures and microchannels in the shear failure zone of the reservoir. The most popular method for calculating the fluid saturations in the reservoir is material balance method.

Arthur et al. (1991) proposed a technique for calculating the reservoir fluid saturations by using overall material balance in both oil and water. Tamim and Farouq Ali (1995) developed two different schemes to calculate the reservoir fluid saturations which are used in the present model.

In the first scheme, an overall material balance of only water in both the hot and warm zones are considered. The following general equation is used to calculate the initial mobile fluid saturations.

$$\begin{aligned} \text{Initial mobile fluid} &= \text{initial volume} + \text{injected volume} + \text{cum. inflow} \\ &\quad - \text{cum. Production} - \text{cum. outflow.} \end{aligned} \quad (3.12)$$

The following simple material balance equations are used to calculate the saturation values.

$$S_{w1} = S_{wc} + (S_{wm1} \phi V_{hot} - q_{w1} + q_{w2}) / (\phi V_{hot}), \quad (3.13)$$

$$S_{w2} = S_{wc} + (S_{wm2} \phi V_{warm} - q_{w2}) / (\phi V_{warm}), \quad (3.14)$$

$$S_{o1} = 1 - S_{w1}, \quad (3.15)$$

$$S_{o2} = 1 - S_{w2} \quad (3.16)$$

Where S_{wm1} and S_{wm2} are the initial mobile water saturations in the hot and warm zones, respectively.

In the second scheme both the oil and water material balance are considered. The continuity equation is used to develop the saturation equations by assuming the change in hot zone volume to be equal to the change in warm zone volume.

For both the schemes, the maximum value of hot zone water saturation was restricted to $(1 - S_{or})$ and the mobile water saturation was restricted to $(1 - S_{or} - S_{wc})$ respectively. The details of saturation equations presented by Tamim and Farouq Ali (1995) are shown in the Appendix D.

3.6 Calculation of Average Viscosity

In cyclic steam stimulation process, the productivity of oil mostly depends on the viscosity of the reservoir oil. The viscosity of oil is decreased by injecting steam into the reservoir. As a result the mobility of reservoir fluid increases. Owens and Suter (1965) proposed a viscosity-temperature relationship to calculate the oil viscosity but it over estimates the oil production.

Tamim and Farouq Ali (1995) developed an improved analytical method to calculate the viscosity of the reservoir fluids. In their approach actual area-weighted averages of the oil and water viscosities were calculated by using average temperatures of the hot and warm zones. A correlation was developed between the average temperatures and the average viscosities. This new approach is used for calculating viscosity of the reservoir fluids in the present model.

$$\mu_{ave} = \frac{A_1\mu_1 + A_2\mu_2}{A_t} \quad (3.17)$$
$$(A_t = A_1 + A_2)$$

This equation calculates the viscosity values of the reservoir fluids successfully over the wide variation of temperatures.

3.7 Calculation of Relative Permeabilities (Pseudo-relative Permeability)

Change of absolute permeability is not an unusual phenomena in cyclic steam stimulation process. Because the fractures and microchannels are created in the shear failure zone of the heavy oil reservoir during steam injection period. It is reported in the literature that the effective permeability is increased by two to three order of magnitude in CSS process (Settari et al., 1993).

Settari et al. (1993) considered two main parameters affecting water relative permeability for a porous media with shear planes, namely the conductivity and connectivity of the planes. Also the planes may be bent or curved and they may have branches. The water saturation inside the shear planes can vary from the native water saturation to a very high value. Under these conditions, analytical formulation of the capability of flow path to injection and production of fluid is difficult.

In the present study, an empirical formula (Settari et al., 1993) has been developed to calculate the enhanced oil and water relative permeabilities. Pethrick et al. (1988) proposed a set of saturation dependent relative permeability values found from experiments for simulation of the Wolf Lake project. For calculating pseudo-relative permeabilities in shear failure zone of the reservoir, this values of water-oil relative permeabilities are used as the original reservoir permeability. There are two methods of obtaining an empirical correlation; multiplication of the original relative permeability or by two sets of relative permeabilities (Settari et al., 1993). The proposed empirical formulas are:

1. Multiplication approach:

Assume that the k_w and k_o in fully failed zone is a product of a multiplier, X_w and X_o , and the original relative permeability, k_{rw} and k_{ro} . Then for a reservoir failed to a certain degree f , the pseudo-relative permeability of water and oil are

$$k_{rw}^* = (1-f) \times k_{rw} + f \times X_w \times k_{rw} \quad (3.18)$$

$$k_{ro}^* = (1-f) \times k_{ro} + f \times X_o \times k_{ro} \quad (3.19)$$

2. Two sets of relative permeability approach:

In this approach the relative permeability table for fail sand $k_{rw, fail}$ is developed independently. Then the pseudo-relative permeability to water and oil are

$$k_{rw}^* = (1-f) \times k_{rw} + f \times X_w \times k_{rw, fail} \quad (3.20)$$

$$k_{ro}^* = (1-f) \times k_{ro} + f \times X_o \times k_{ro, fail} \quad (3.21)$$

where X is the multiplication factor to relative permeability to water and oil. In the field, the flow behavior during the early production is characterized by a very high water cut with a trace of oil production. This period corresponds to a high K_{rw} multiplier because the heterogeneously created flow paths still remain open. When the pore pressure is further reduced, the paths are partially closed or the connections between start to break. This is the end of the initial flow back of water and start of oil production. The high K_{rw} multiplier starts to reduce to its original value. Figure 3.2 shows the pressure dependent multiplication factor to relative permeability to water and oil. The degree of failure f is defined by linearly interpolating in the failure zone between higher and lower pressure limit. At lower pressure, where failure has not started, $f = 0.0$ and for fully failed zone where pressure is high enough, $f = 1.0$ is considered. Figure 3.3 shows the relationship between degree of failure and reservoir pressure during production periods. The pseudo-relative permeabilities depend on the saturation and pressure in the failure zone of the reservoir. Since the flow of two phase is considered in this model so only the multiplication approach is currently used. Pseudo-relative permeability to gas phase is not considered, because the mobility of steam is naturally high and the growth of steam zone is controlled primarily by energy flow. Details of the above equations are presented in the Appendix E.

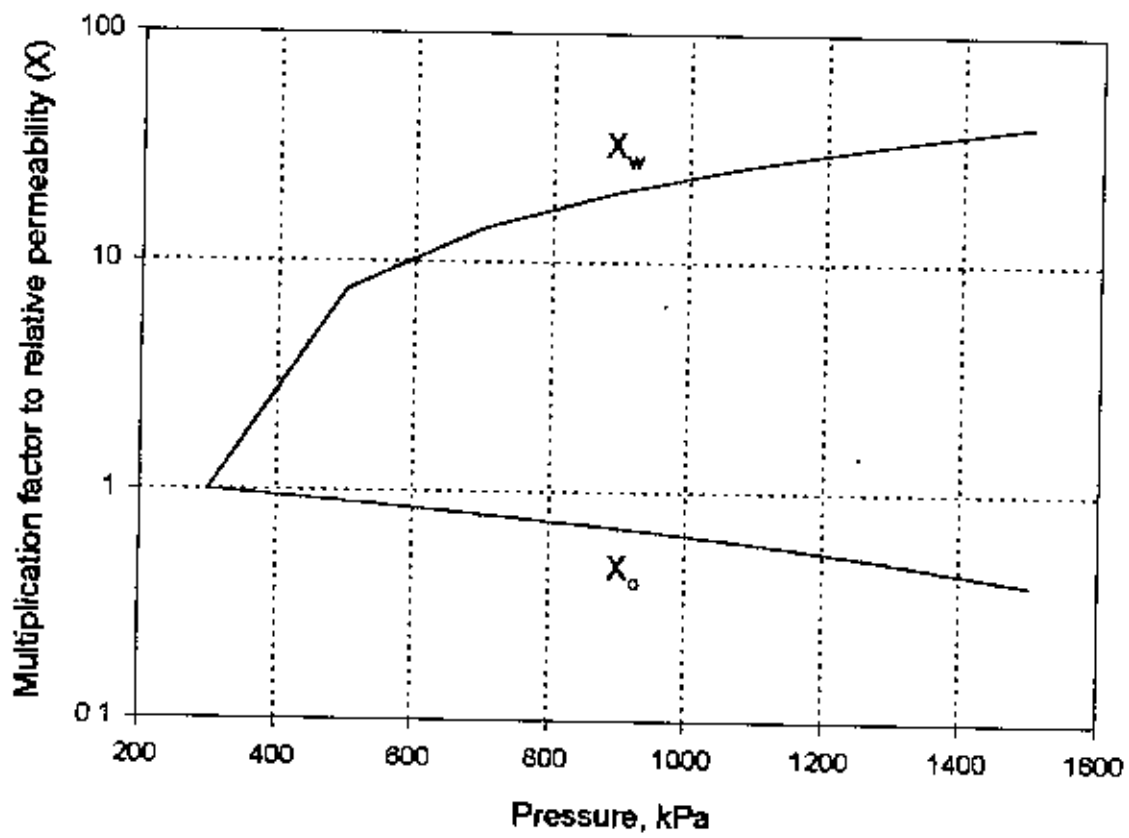


Figure 3.2- Multiplication factor to relative permeability to water and oil.

Since the pseudo-relative permeability is derived from the geomechanical findings of the reservoir, the model should have some features such as local dependency and directional dependency.

Local dependency: The width, geometry, branches and straightness of the fractures are major factors for the flow capability of paths in the shear failure zone. All of these factors can change from location to location. Therefore, the defined pseudo-relative permeability for the shear failure zone must be locally dependent.

Directional dependency: The multiple planes in shear failure zone may have a preferred orientation, so the pseudo-relative permeabilities should be directional. For example, enhanced water permeability will not be expected in a direction perpendicular to the shear planes.

The pseudo-relative permeability in the failure zone is influenced by the location of the reservoir as well as direction of the shear plane. These effects are calculated by the second part of Equation 3.18 and 3.19.

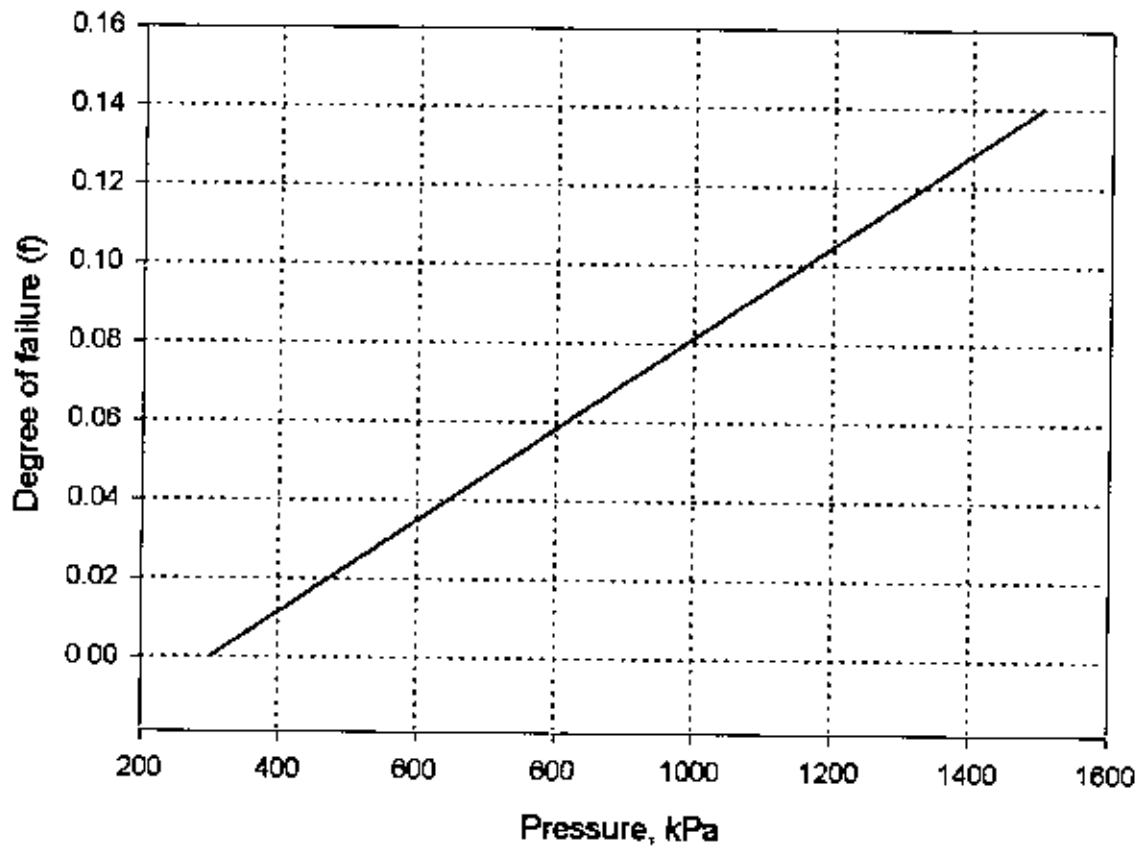


Figure 3.3 - Degree of failure with reservoir pressure.

Chapter IV

COMPUTER IMPLEMENTATION

To calculate the oil and water production rate from this new model developed in the previous chapter, a FORTRAN program was written. The main program is divided into subroutines and also looped with eighth cycles of operation. The pseudo-relative permeability values are calculated by using correlations and tabulated values of relative permeability. For the case of intermediate values of tabulated data, cubic spline interpolation method is used. A data file is used for all the necessary data in the main program. A time step size of two days are used for all the production cycles. At the end of every cycle the production results are written and updated. The program is repeated after all the cycles. The steps to be followed are described in the next paragraph.

4.1 Model Description

1. In CSS process, steam is injected into the reservoir high enough (above fracture pressure) pressure to create shear failure zone. The extent of shear failure zone is determined by using Wheeler's (1969) material balance equation (Equation 3.6).
2. The shear failure zone is divided into two concentric elliptical cylinder on the basis of isotherm. The hot zone is extended up to the 100°C isotherm and warm zone is extended up to the drainage boundary ($16 + 0.01^{\circ}\text{C}$) of the reservoir (Figure 3.1).
3. The average reservoir temperature is determined at the end of injection period throughout the length of isotherm.

4. The heat loss by conduction to the over and underburden during soak and production period is determined. By using energy balance equation the average zone temperature is determined.
5. The pseudo-relative permeability values are determined by using correlations and tabulated values of water-oil relative permeability.
6. The fluid production rate from the hot and warm zone is calculated by using flow rate equations. The wellbore fluid height is considered zero at all time and interface fluid height is calculated by using material balance equation.
7. The residual heat remaining in the reservoir at the end of a cycle is added to the beginning of the next cycle.

4.2 Subroutines Used by Main Program

The following subroutines are used by the main program to implement the ideas of the model and described in a sequential order. A flow diagram of the computer program is shown in Figure 4.1.

4.2.1 Initialization of the program

DATAIN

DATAIN is the first subroutine. It contains all the necessary input data that are used in the main and sub program. It has five sets of input data and all are in SI units. The injection, soak and production times for each cycle with steam pressure, saturation temperature and fluid loss coefficient are contained by the first set. The second set

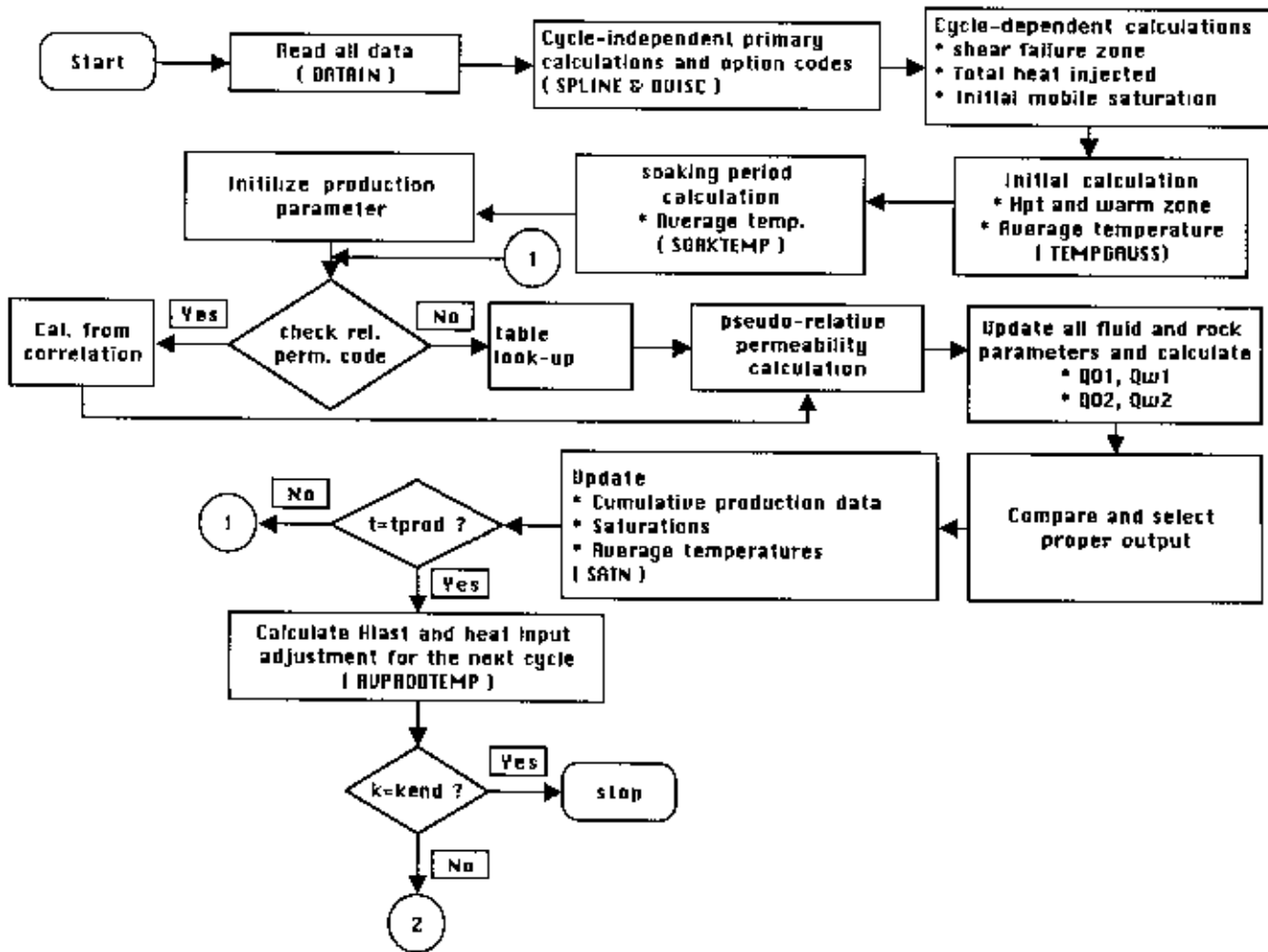


Figure 4.1-Computational Flow Diagram of the Model

contains the physical parameters of the reservoir and steam like porosity, formation thickness, injection rate, steam quality, absolute permeability and initial reservoir temperature. The third set composed of compressibilities, saturations and initial reservoir pressure. Thermal conductivities and heat capacities of the reservoir are provided in the fourth set. The all relative permeability values are included in the fifth set.

SPLINE

The intermediate values of the tabulated relative permeabilities are calculated by this subroutine.

OVISC

This program calculates the oil and water viscosities and densities. Here the viscosity values are determined at the initial reservoir temperature.

4.2.2 Subroutines of injection period

Subroutines of this group are used for the initialization of the project and cumulative values. The maximum and minimum production limits are set at this stage and also the cycle calculations are initialized.

PVTIN

This subroutine is used for the calculation of viscosity, density and heat capacity of steam, water and oil and also the latent heat of vaporization. Here all the calculations are based on the steam temperature.

TEMPGAUSS

It is one of the most important programs, which calculates the hot and warm zone boundaries and also the extent of shear failure zone. Wheeler's (1969) material balance equation is used for calculating fluid leak-off velocity. This is accomplished by using numerical integration. The average zone temperatures are also calculated here and the heat remaining in the previous cycle is added to the heat input to the next cycle.

PRESSURE

The name of this subroutine implies that it calculates the hot and warm zone interface pressure and also the outer boundary pressure.

4.2.3 Subroutines of Soak Period

SOAKTEMP

This program is used for the calculation of heat loss to the over and underburden during soak period. It also calculates the average temperature of the reservoir during soak period. At this stage the main program calculates the initial mobile saturation and PVT data. The oil in place is estimated here and the production stage of the calculation is initialized.

4.2.4 Subroutines of Production Period

Before the start of production period, the relative permeabilities and the mobilities of the reservoir fluids are determined. The pseudo-relative permeability values are calculated by using correlations and tabulated values of the permeability data. Then the flow rates are calculated and the limits are checked. Finally cumulative values are updated.

SATN

During production stage, the saturation values are calculated by this program. This calculated values are used for the next time step. Also the production results are written here.

AVPRODTEMP

This program is used for the calculation of average reservoir temperature during production period. It also calculates the heat loss to the over and underburden through fluid production.

Chapter V

RESULTS AND DISCUSSION

Performance of a Cyclic Steam Stimulation (PCSS) process including a shear failure zone around the wellbore is predicted in this study. An extensive analysis has been done with this new analytical model. Pseudo-relative permeability functions are used for the simulation of shear failure zone in the reservoir. The model also accounts for flow rate in an elliptical heated zone geometry.

An extensive sensitivity study has been conducted to verify the effectiveness, as well as limitations of this pseudo-relative permeability model. The effects of changes in the soak time, steam volume, time step size, steam temperature, steam quality and reservoir thickness are discussed here.

In this chapter, the sample results are discussed and analyzed for the above mentioned aspects of the CSS process. The main objective is to explore and understand CSS oil recovery process using pseudo-relative permeabilities for simulating the shear failure zone.

5.1 Simulation Data

The data used for this simulation work is the published data (Pethrick et al., 1988) on the Wolf Lake project, owned by BP resources Canada Limited. The simulation input data are shown in Table 5.1 and the oil-water relative permeabilities are shown in Table 5.2. The operational data are shown in Table 5.3. Some of the correlations used for the purpose of determining fluid properties are presented in Appendix F.

All the eight cycle results are used for the investigation and sensitivity study. For analyzing the results, several production performance parameters are used. These are the oil-steam ratio (OSR), calendar day oil rate (CDOR) and water-oil ratio (WOR).

Table 5.1 - Simulation input data.

Porosity,	fraction	0.305
Permeability,	μm^2	1.0
Initial reservoir pressure,	kPa	2750.0
Initial oil saturation,	fraction	0.66
Initial reservoir temperature,	$^{\circ}\text{C}$	16.0
Irreducible water saturation,	fraction	0.34
Residual oil saturation,	fraction	0.35
Rock compressibility,	kPa^{-1}	0.45E-6
Water compressibility,	kPa^{-1}	0.45E-6
Oil compressibility,	kPa^{-1}	0.34E-6
Oil thermal expansion coefficient,	$^{\circ}\text{C}^{-1}$	0.848E-3
Reservoir specific heat,	$\text{kJ m}^{-3}\text{K}^{-1}$	2350.0
Reservoir thermal conductivity,	$\text{kJ m}^{-1}\text{d}^{-1}\text{K}^{-1}$	149.6
Cap/base rock specific heat,	$\text{kJ m}^{-3}\text{K}^{-1}$	2350.0
Cap/base rock thermal conductivity,	$\text{kJ m}^{-1}\text{d}^{-1}\text{K}^{-1}$	149.6
Oil viscosity at 16 $^{\circ}\text{C}$,	mPa.s	81000.0
Oil viscosity at 100 $^{\circ}\text{C}$,	mPa.s	115.0
Oil viscosity at 200 $^{\circ}\text{C}$,	mPa.s	6.8
Net pay,	m	23.8
Fracture half length,	m	240.0

Table 5.2 - Water-oil relative permeability (Pethrick et al., 1988)

S_w	k_{rw}	k_{ro}
0.3200	0.0000	1.0000
0.4300	0.0025	0.6440
0.5450	0.0100	0.3910
0.5929	0.0200	0.2420
0.6359	0.0330	0.1380
0.6760	0.0530	0.0610
0.7145	0.0730	0.0300
0.7530	0.1130	0.0120
0.7700	0.1200	0.0000

Table 5.3 - Operational data

Cycle	Steam Slug Size (m ³)	Injection Time (days)	Soak Time (days)	Production Time (days)	Cycle Time (days)
1	6250	25	15	89	129
2	7000	28	15	123	166
3	7500	30	15	135	180
4	8000	32	15	150	197
5	8250	33	15	161	209
6	8500	34	15	174	223
7	8750	35	15	188	238
8	9000	36	15	202	253

5.2 Elliptical Flow into a Well

The results obtained from this pseudo-relative permeability model are shown in Figure 5.1 through Figure 5.7. The results are compared with BP Simulation (BPS) results and conventional method results (Tamim and Farouq Ali, 1995).

The conventional model was developed by Tamim and Farouq Ali (1995). They examined CSS performances under fractured as well as unfractured wellbore conditions. Flow into a completely closed fracture which involves Elliptical Flow into a circular Well (EFW) was investigated. They examined a close-form as well as an approximate solution to this problems. This investigation failed to match the field results. Based on the results of these studies, a partially open fracture was investigated with the help of the new model. This model predicted higher water production compared with simulation results.

The only field data on Wolf Lake project, jointly owned by Petro-Canada and BP Resources Canada Limited, was published by Pethrick et al. (1988). Pethrick et al. (1988) described that fractures were required to achieve reasonable steam injection rates in the field. They optimized the injection and production strategies of individual wells in the Wolf Lake projects. Prior to this optimization, several years of CSS production data from BP's Phase A Pilot in the Wolf Lake project were matched to validate the thermal simulator. The agreement between the simulation results and field behavior allowed a high degree of confidence in the optimization strategy. This data (Pethrick et al., 1988) has been used as the simulation input data in the present pseudo-relative permeability model.

Figure 5.1 shows the cycle oil production along with BPS value and conventional approach. The predicted cycle oil productions match fairly well with BPS value whereas conventional approach produced much lower values. The oil production is nearly same to BPS value upto the sixth cycle but decreases in the next two cycles.

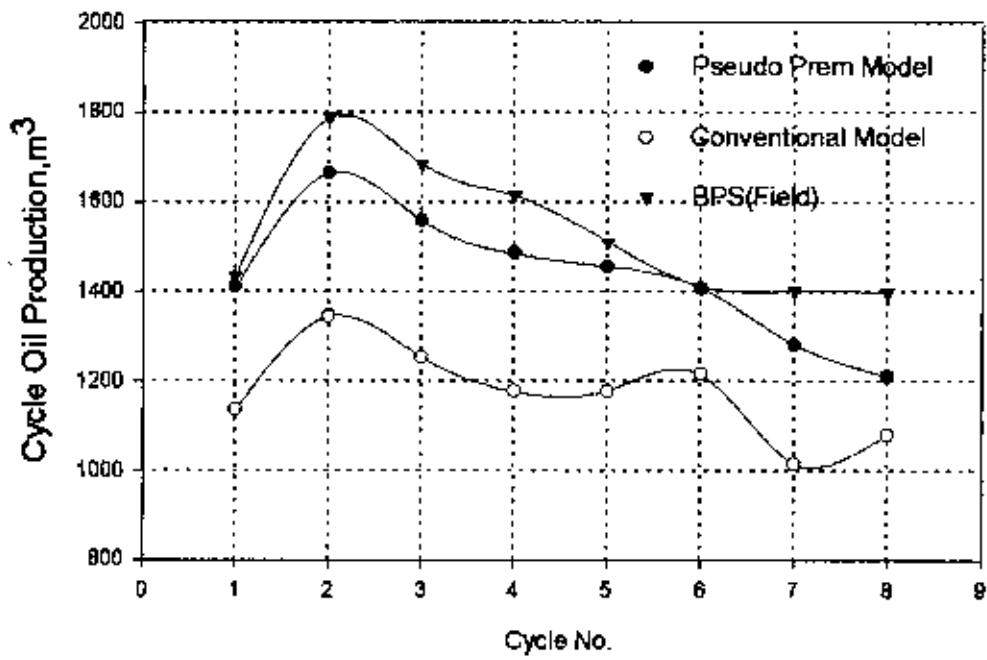


Figure 5.1-Comparison of cycle oil production.

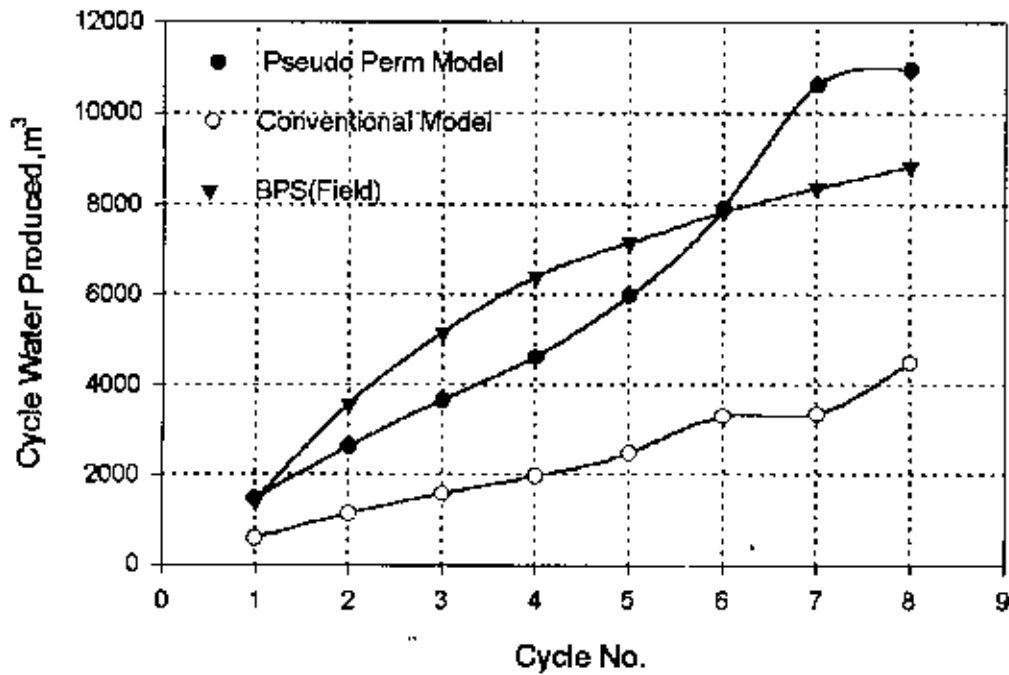


Figure 5.2-Comparison of cycle water production.

The reason could be the decrease of the relative permeability due to the remoulding of fractures and microchannels. So the pseudo-relative permeability model oil production results are more accurate compared to the conventional approach model. Cycle water production predicted by the conventional model was also very low as was the case for the oil production. The pseudo-relative permeability model improved this situation significantly. Figure 5.2 shows this results. As a consequence to lower oil production in the last two cycles, water production was higher. In the eighth cycle, the pseudo-relative permeability model produced 2000 m³ of more water than BPS results. Both oil and water production increased considerably in the pseudo-relative permeability model due to the use of enhanced permeability, which was created by the shear failure zone. As the conventional model did not consider the shear failure zone, it failed to match the field data. Figure 5.3 shows the cumulative oil production. It can be seen that the cumulative oil production curve follows approximately the same path as BPS value whereas the conventional model is always well below the pseudo-relative permeability curve. The cumulative water productions are shown in Figure 5.4. It is seen that the cumulative water production is slightly less than the BPS value in the middle of the cycles. At the end of eighth cycle the cumulative water production is approximately same as the BPS value. Compared to the pseudo-relative permeability model the conventional model produces much less water. At the end of eighth cycle the pseudo-relative permeability model produces 47873 m³ of water whereas conventional model produces only 18930 m³ of water. Figure 5.5 shows the cycle oil-steam ratio (OSR). It is seen that the cycle oil-steam ratio closely matches with BPS values. The cycle oil-steam ratio is approximately same as the BPS value upto the sixth cycle and then decreases. At the end of eighth cycle, the OSR is 0.143 whereas BPS value is 0.156. The conventional model produced much less OSR compared with pseudo-relative permeability model. Figure 5.6 shows the cycle water-oil ratio (WOR). It is seen that the cycle WOR closely matches with BPS value up to the sixth cycle. After sixth cycle the WOR increases sharply. At the end of eighth cycle the pseudo-relative permeability model produces WOR is 9.06 whereas BPS produces 6.31. The reason is the high water cut occurred in the later cycle from failure zone. The conventional

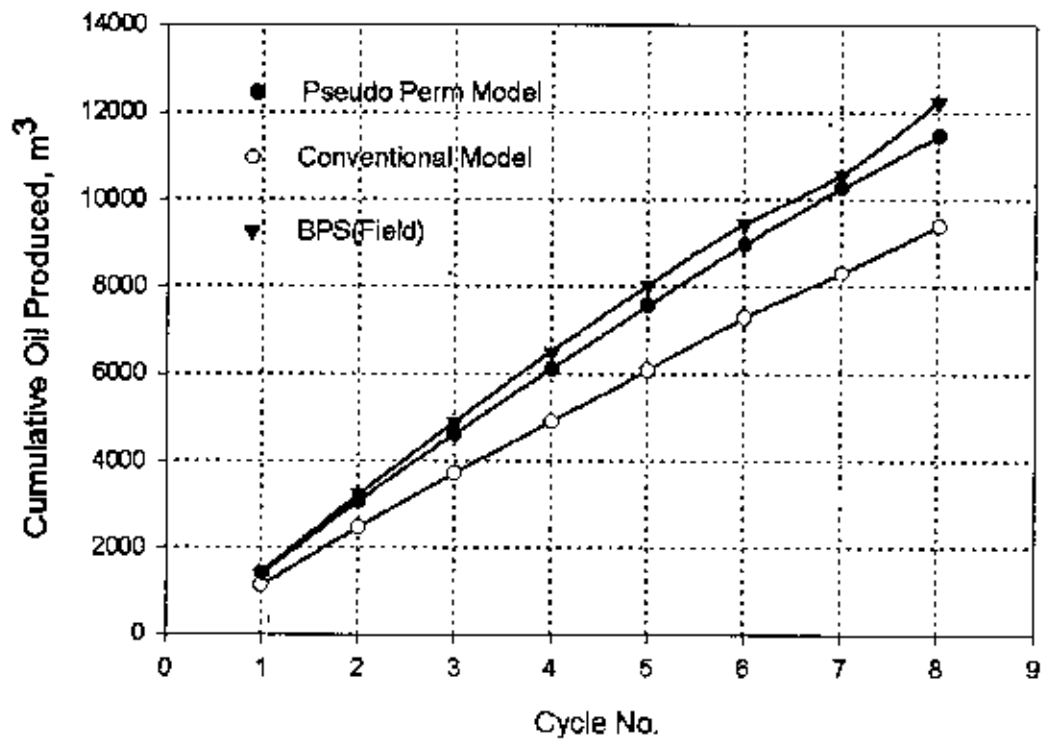


Figure 5.3-Comparison of cumulative oil production.

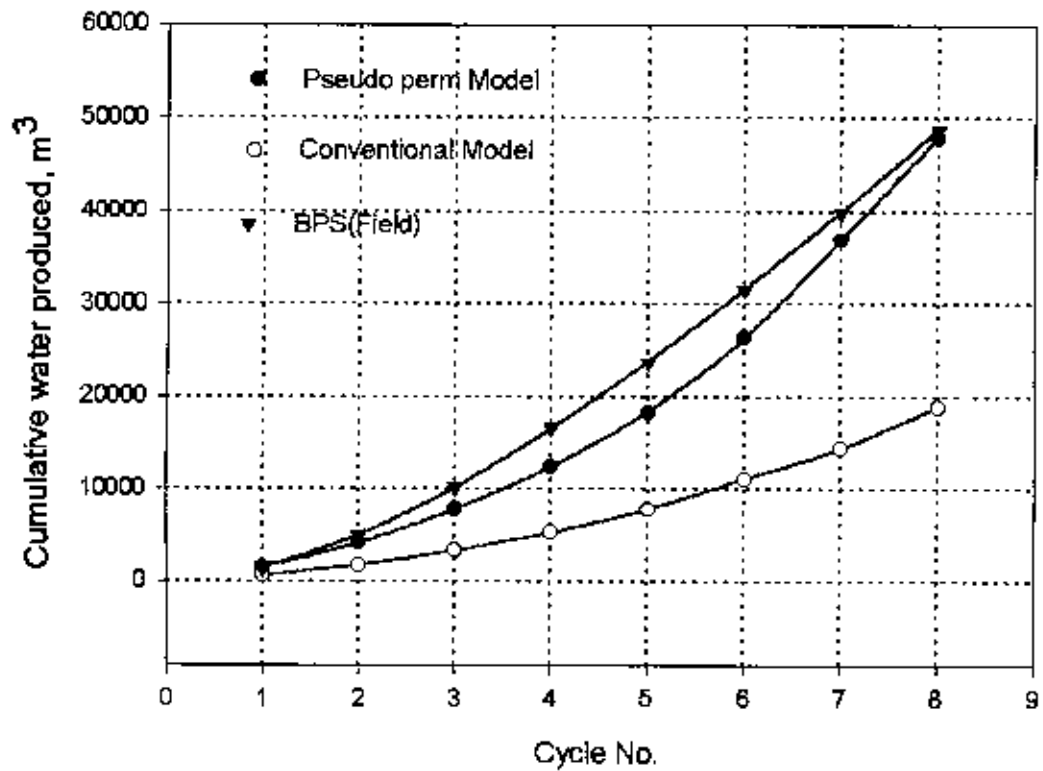


Figure 5.4-Comparison of cumulative water production.

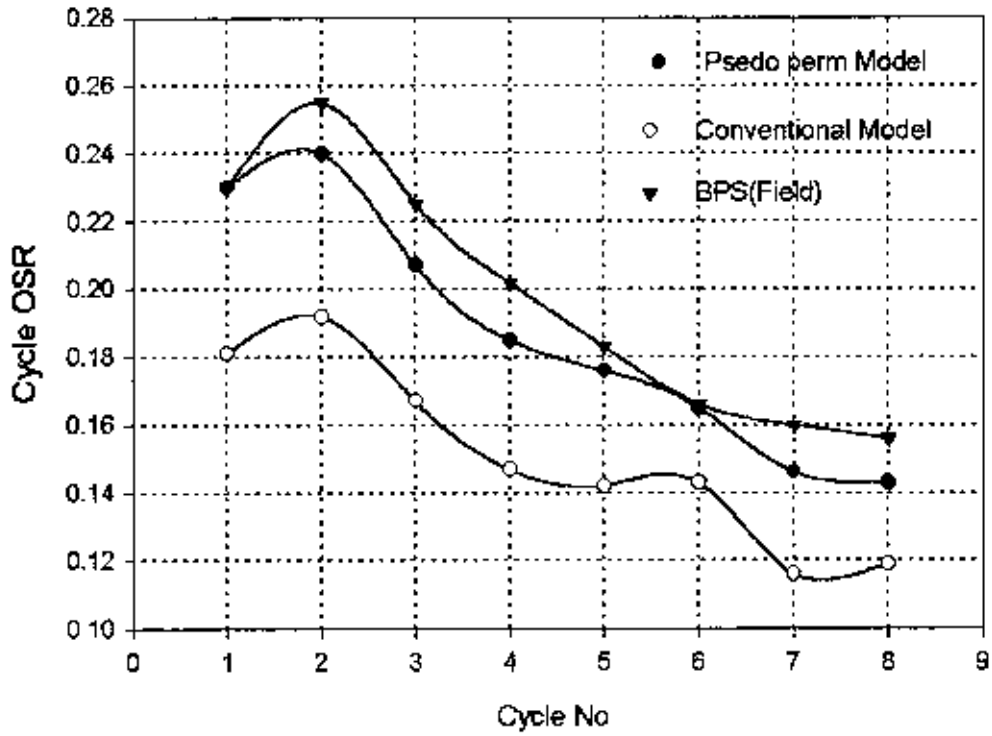


Figure 5.5-Comparison of cycle oil-steam ratio.

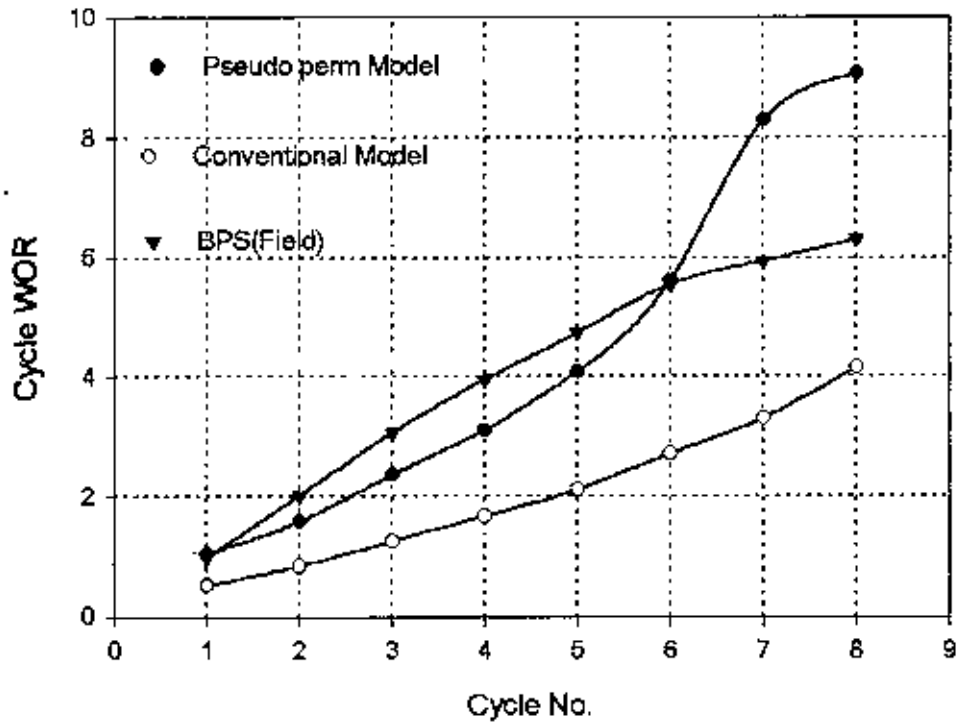


Figure 5.6-Comparison of cycle water-oil ratio.

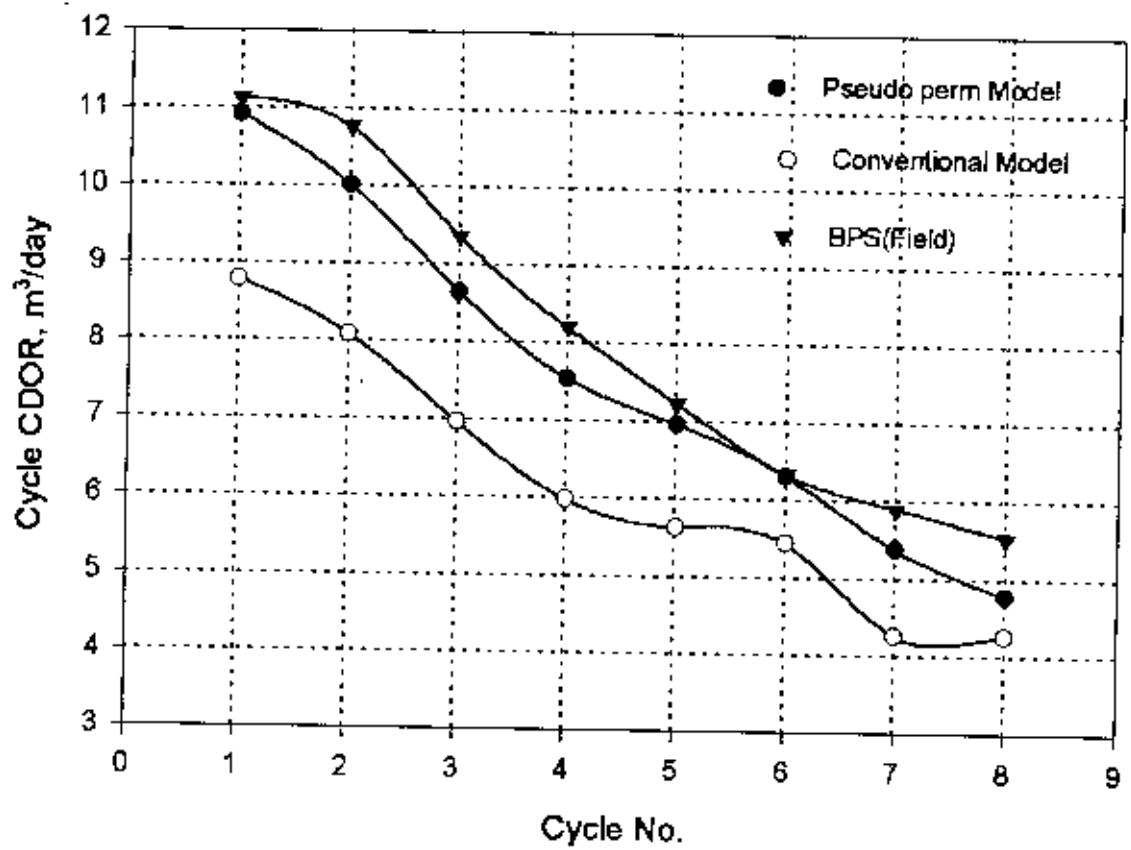


Figure 5.7-Comparison of calendar day oil production rate

model produces less cycle WOR than the pseudo-relative permeability model. The cycle calendar day oil rate (CDOR) is shown in Figure 5.7. It is seen that the cycle CDOR points close are fairly close to the BPS values. The conventional model produced much lower cycle CDOR than pseudo-relative permeability model. It is seen that the difference is more in the early cycles and less in the later cycle.

It is seen that the results of the production performance parameters closely matched with results published by BP Resources Canada Limited (Pethrick, et.al.,1988). A little amount of discrepancies appeared in the case of cycle oil and water production but the cumulative values of oil and water production matched fairly well. The other performance parameters like OSR, WOR and CDOR give much better results than the conventional model. The predicted results indicate that fractures and microchannels are created in the shear failure zone of the heavy oil reservoir during steam injection period. This enhanced the permeability of the reservoir. The flow rate of the reservoir fluids in CSS process depends on the permeability of the reservoir. This model accounts the actual permeability of the reservoir by using pseudo-relative permeability functions. The predicted results matched fairly well with field performance results (BPS), due to the calculation of enhanced permeability and flow rate. It can be said that this work represent the actual flow geometry and shear failure criteria in heavy oil sands for CSS operation. That is, the fractures and microchannels are created in the shear failure zone of reservoir, during injection period, remain during production period. The shear failure phenomena of heavy oil reservoirs in CSS process can be successfully simulated by using pseudo-relative permeability functions.

5.3 Sensitivity Study

The pseudo-relative permeability model is used successfully to simulate the shear failure condition of heavy oil reservoirs in CSS process. A sensitivity analysis has been

made to determine the acceptable range of operation of this new analytical model. Several physical and operational parameters were selected for the sensitivity analysis.

5.3.1 Effects of Soak Time

The selection of soak period is an important factor for cyclic steam stimulation process. Some authors have found that presence of any soak period does not affect the production, on the other hand some have suggested an optimum duration for soaking. There is no fixed guideline for setting the actual soak period. A minimum of 2 to 3 days are needed to change the well head assembly from injection to production. Figure 5.8 shows the cycle oil production for different soak periods. The 10 days soak period produces little more oil in the early cycles than later cycles compared with the base soak time of 15 days. On the other hand, the 20 days soak period produces less oil in the early cycles and more in the later cycles. This is due to more available oil and late heating of the formation. There is little difference of cycle oil production in various soak periods. So the soaking period between 10 to 20 days shows better result. Figure 5.9 shows the cumulative oil production for different soak periods. The total oil production has no effect for different soak periods. The cycle water productions for different soak periods are shown in Figure 5.10 and the cumulative water productions are shown in Figure 5.11. The cycle and total water production also do not change for different soak periods. It is seen that the duration of soak period has no major effects on production performance parameters but longer soak period increases the heat loss to the over and under burden by conduction. The conduction heat loss decrease the production performance. It can be said that the 15 days soak period is better for history matching of production performance.

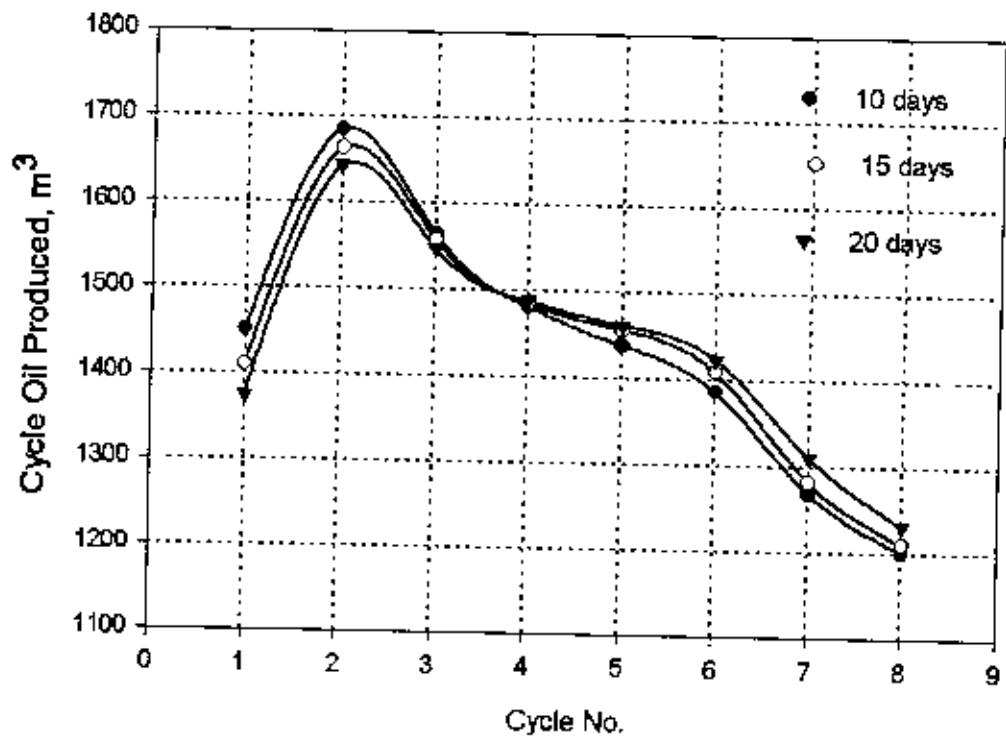


Figure 5.8- Oil production at each cycle for different soak periods.

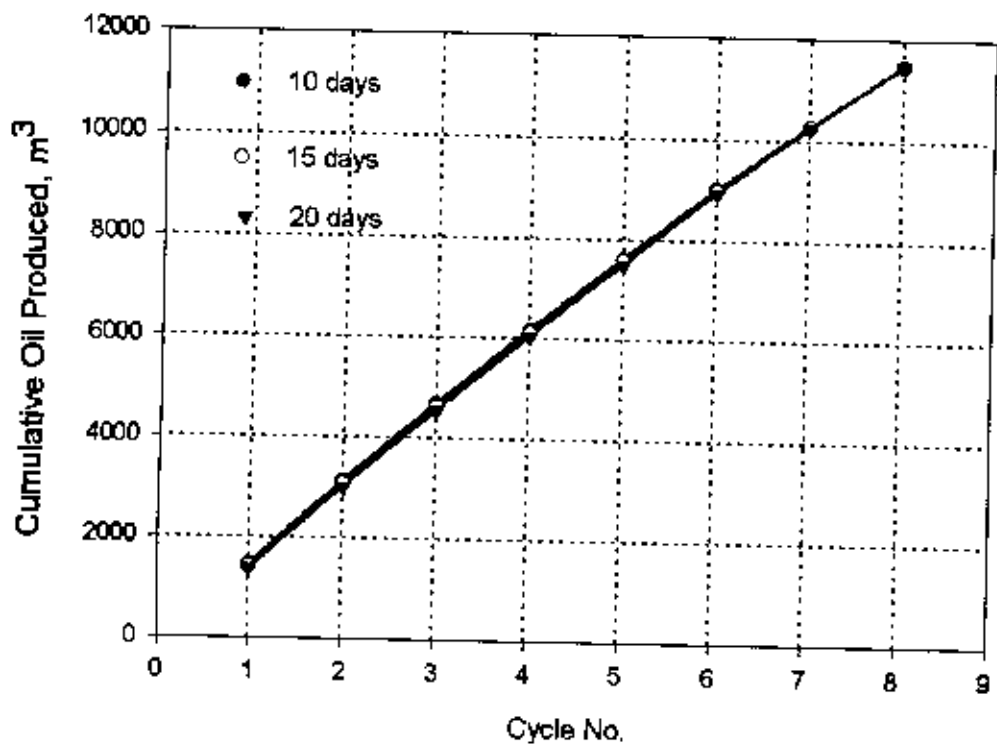


Figure 5.9- Cumulative oil production for different soak periods.

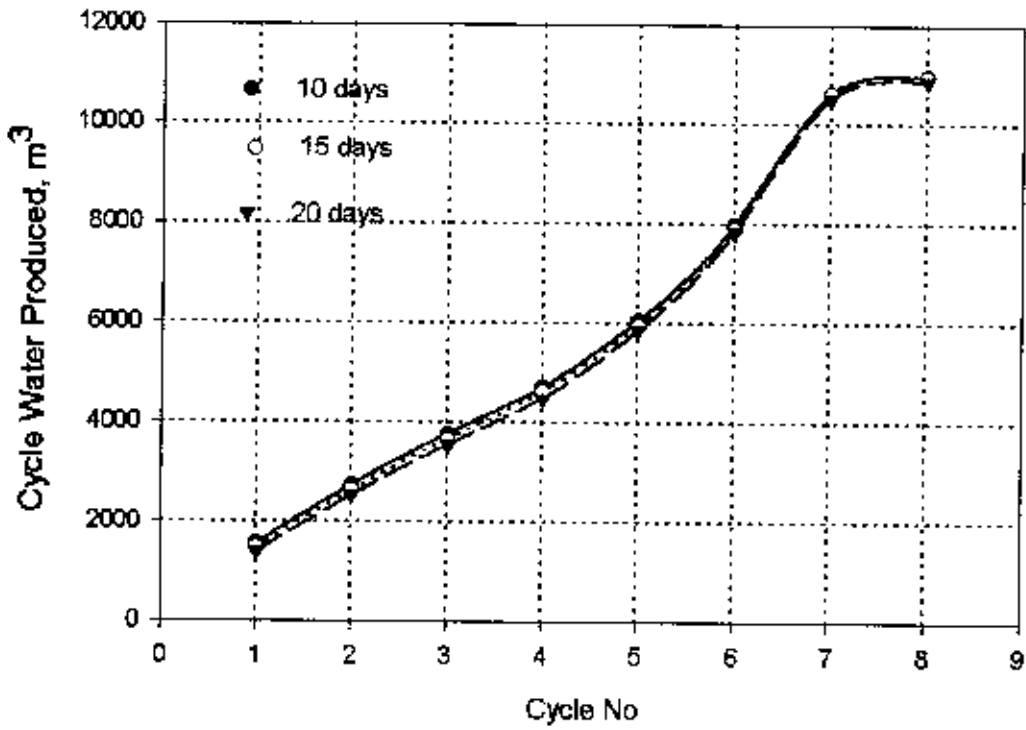


Figure 5.10- Water production at each cycle for different soak periods.

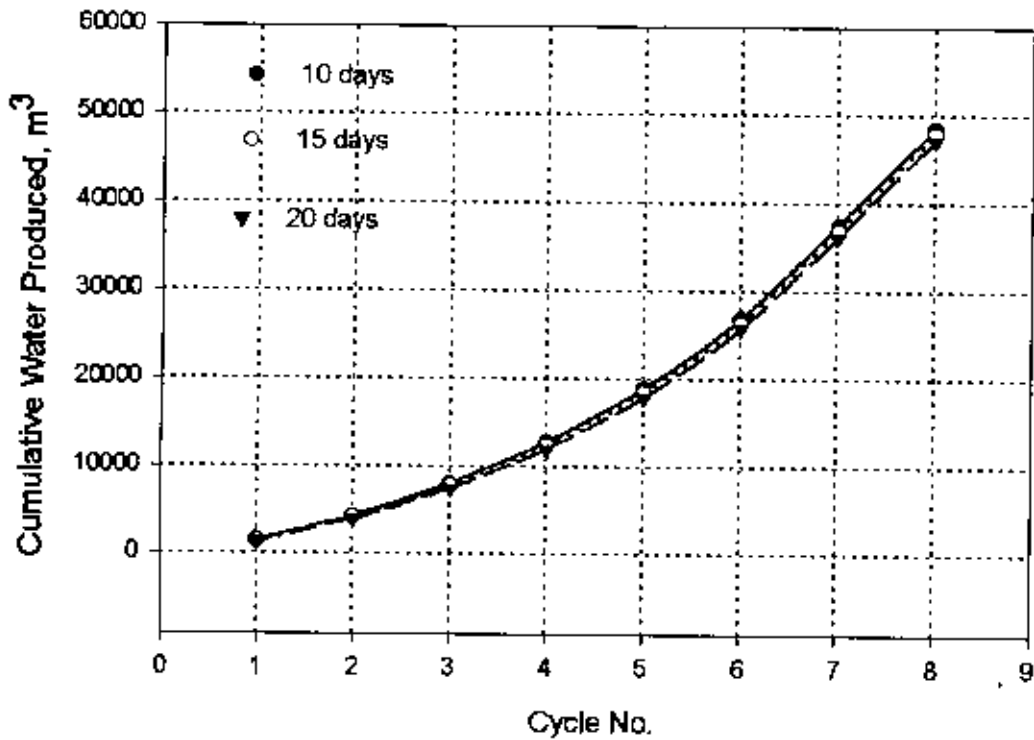


Figure 5.11- Cumulative water production for different soak periods.

5.3.2 Effects of Steam Injection Rates

The steam injection rate significantly affects the productivity of cyclic steam stimulation process in heavy oil reservoirs. Higher injection rate produce more oil due to the injection of more heat and it capture more drainage area. Economic factors play an important role in steam injection strategy. Increased steam production involves higher boiler capacity and higher operational costs. Steam injection rates should be based on cost per cubic meter of oil produced. Figure 5.12 shows the cycle oil productions for various steam injection rates. The injection rates of 200 m³/day produces much less oil than the base rate of 250 m³/day in the later cycles. The injection rate of 300 m³/day produces much higher oil in later cycles than the early cycles compared with base case. The cumulative oil production has no significant difference in early cycles but the later cycles have little difference for various steam injection rates (Figure 5.13). The cycle water productions for different steam injection rates are shown in the Figure 5.14. The lower injection rate produces much more water than the higher injection rates. Figure 5.15 shows the cumulative water production for various steam injection rates. At the end of 8th cycle the lower injection rate produced 7000 m³ more water than the base case but higher injection rate produced 5000 m³ less water. These results are contrary to the expected results and the actual reason for such behavior could not be understood. The cycle oil-steam ratios (OSR) for various steam injection rates are shown in the figure 5.16. It is seen that the lower injection rate produces less oil-steam ratio than the higher injection rate in the later cycles. At the end of 8th cycle the lower injection rate produced OSR is 0.113 and at the higher rate the ratio is 0.156 whereas the base case produced ratio is 0.143. The cycle calendar day oil production rates (CDOR) have the same trend as the OSR (Figure 5.17). Figure 5.18 shows the cycle water-oil ratio (WOR) for different steam injection rates. It is seen that the lower injection rate produces more WOR than the higher injection rates. At the end of 8th cycle the WOR is 12.37 for lower injection rate and 6.94 for the higher rate. Whereas produced water-oil ratio for the base case is 9.06. Depending on the operational break-even point, field capacity and initial investment, each reservoir would have a

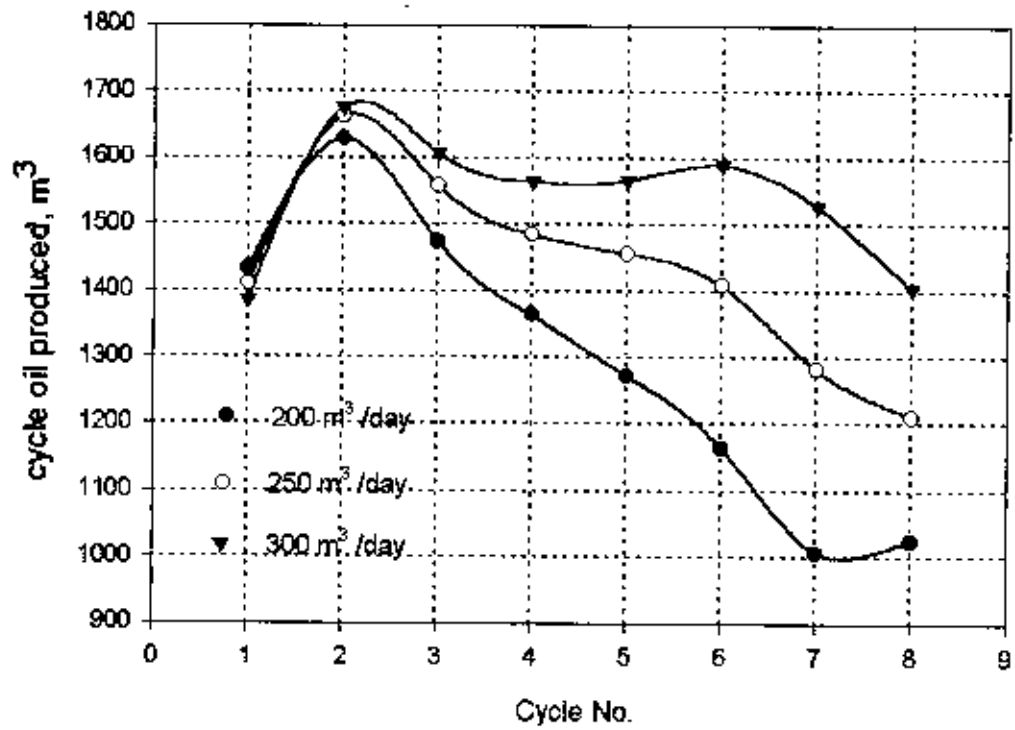


Figure 5.12- Oil production at each cycle for various steam injection rates.

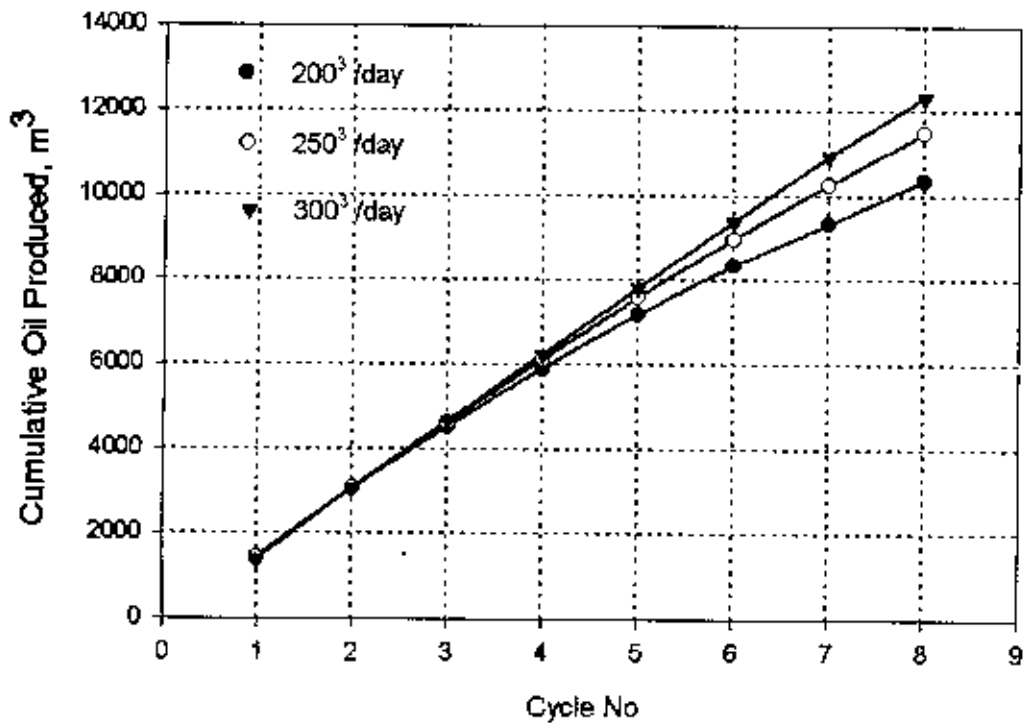


Figure 5.13- Cumulative oil production for different steam injection rates.

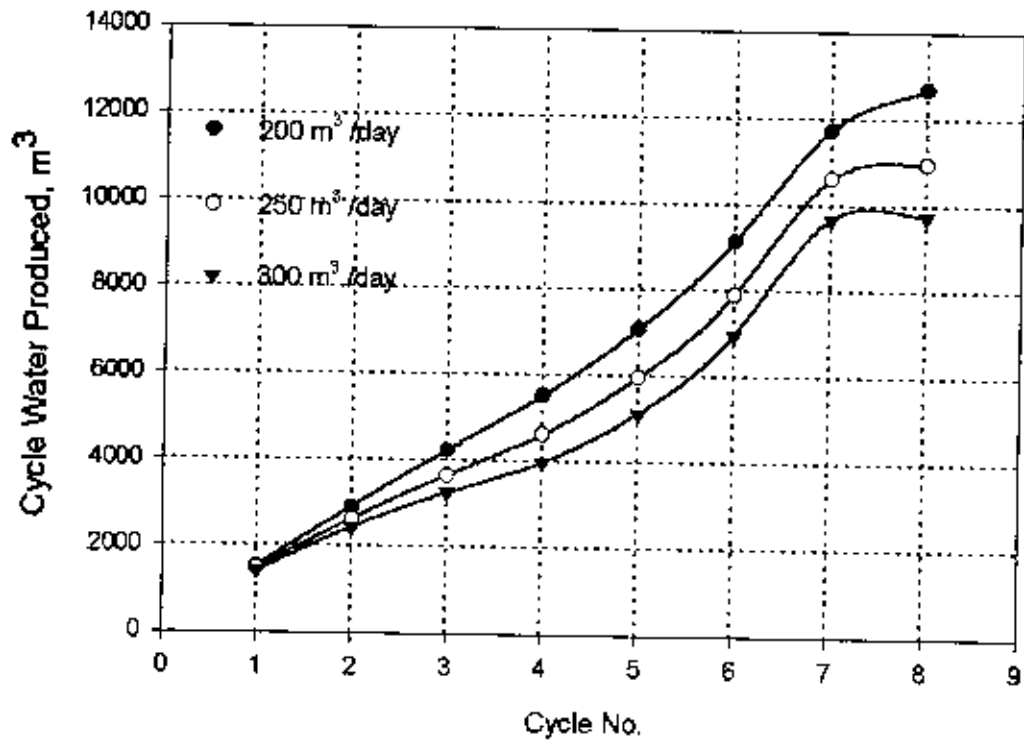


Figure 5.14- Water production at each cycle for different steam injection rates.

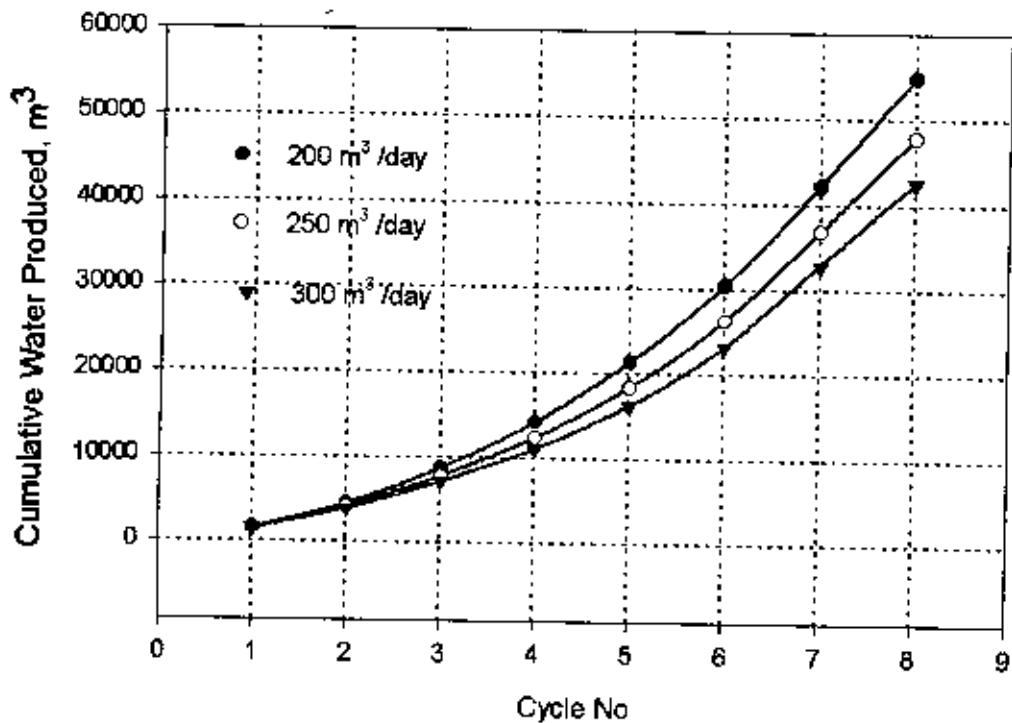


Figure 5.15- Cumulative water production for various steam injection rates.

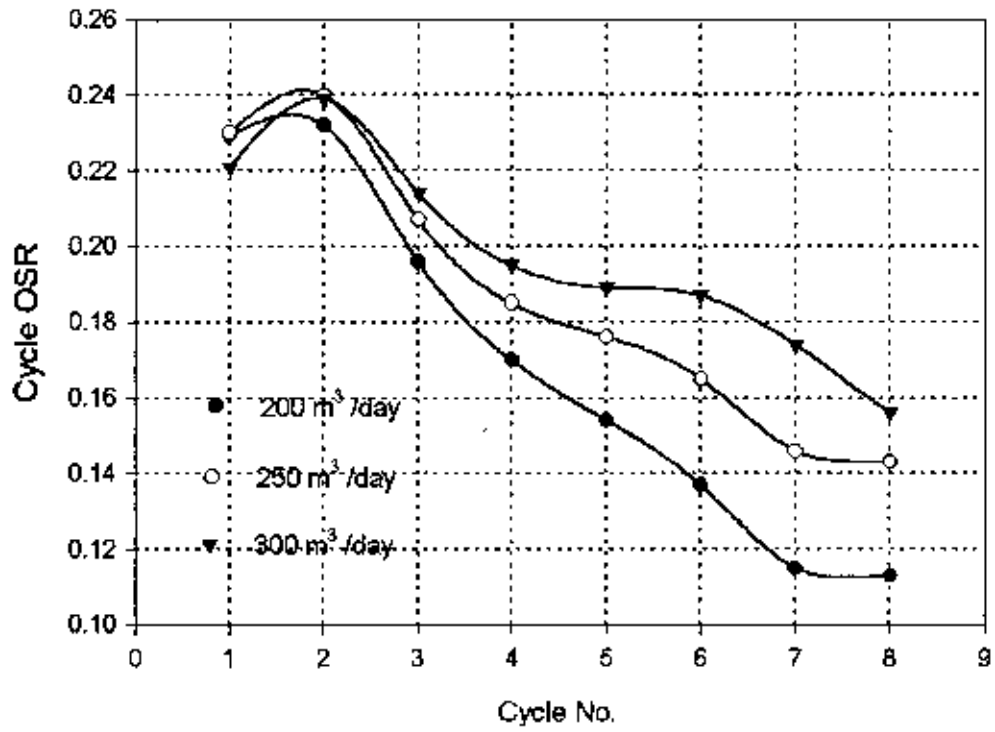


Figure 5.16- Oil-steam ratio at each cycle for various steam injection rates.

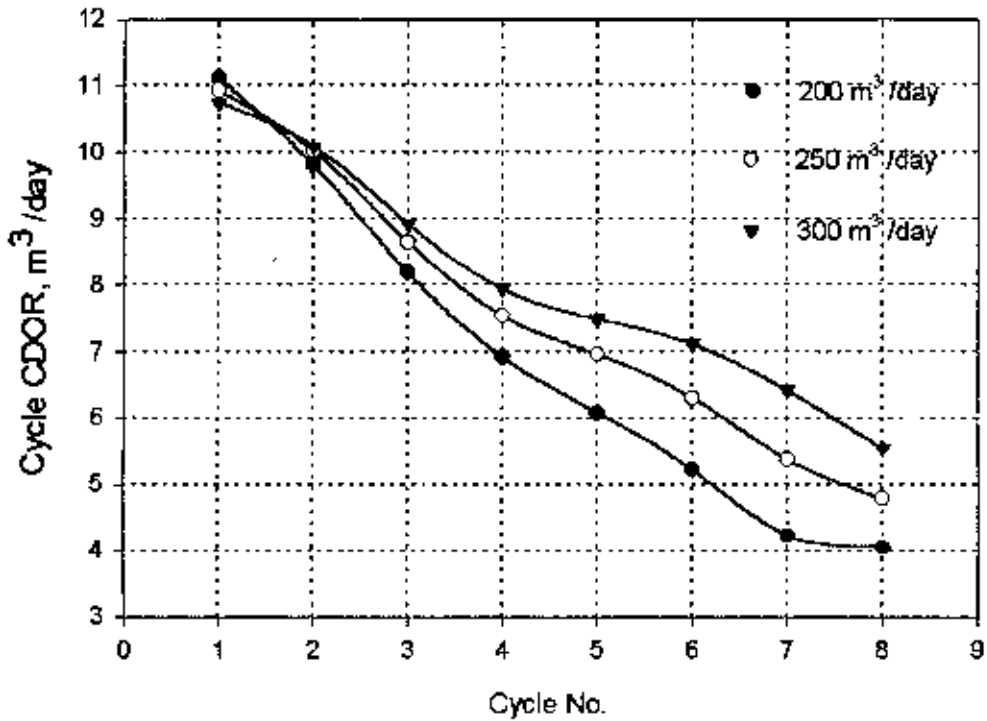


Figure 5.17- Calendar day oil production rates for different steam injection rates.

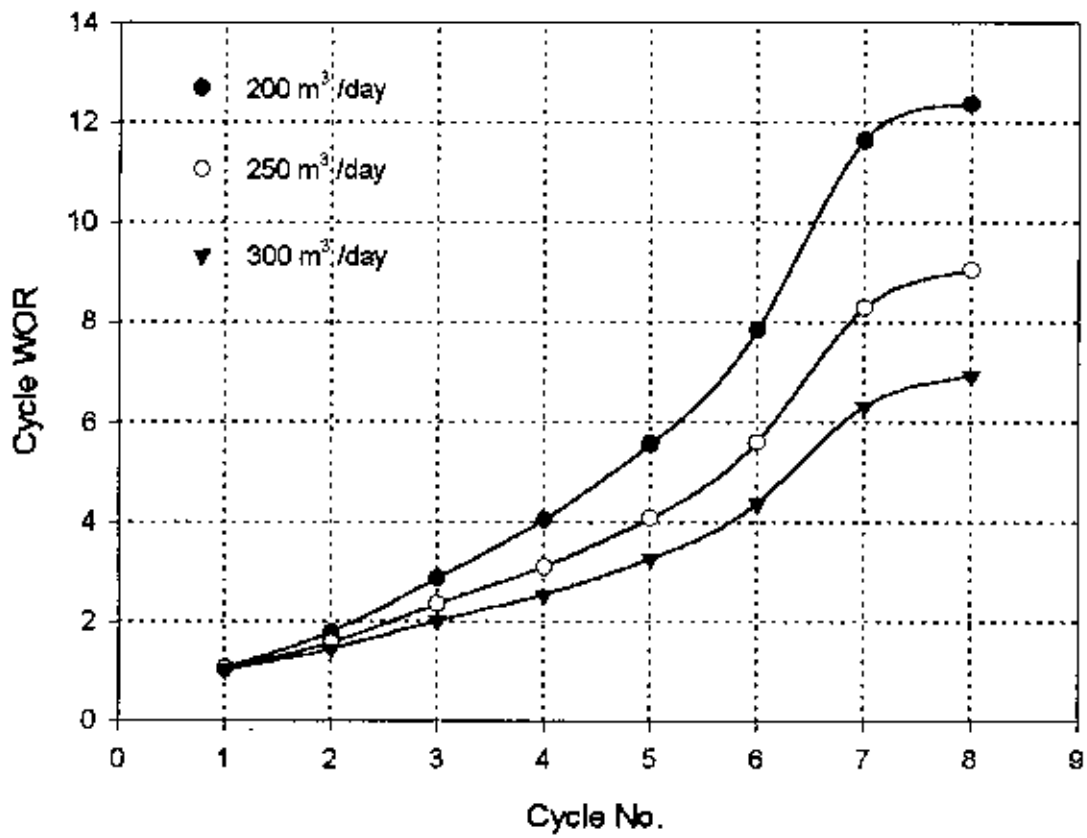


Figure 5.18- Water-oil ratio at each cycle for different steam injection rates.

different optimum strategy. So the setting of steam injection rate $250 \text{ m}^3/\text{day}$ is reasonable for this model and gives better results.

5.3.3 Effects of Time Step Size On Production

The analytical nature of the CSS process shows that the time step size has little effect on production performances. The reservoir temperature decreases with time which decreases the instantaneous flow rate. To accommodate this changing flow rate, temperature and viscosity are calculated at a regular interval during the production cycle. So the time step size affects the viscosity of the reservoir oil. Figure 5.19 shows the cycle oil production for various time step sizes. The 2 days time step size produces slightly less cycle oil than the 5 days and 10 days oil production. Whereas 5 days and 10 days produces approximately same cycle oil. The reason may be the instability of the saturation scheme. The cumulative oil production for various time step sizes are shown in Figure 5.20. It is seen that the total oil production is approximately same for all time step sizes. Figure 5.21 shows the cycle water production for various time step sizes. The 2 days time step size produces approximately same cycle water upto the 6th cycle and picked up in 7th cycle. It produces 2230 m^3 more water than 5 days time step size. The actual reason could not be understood of such behavior in cycle water production. The total water production for various time step sizes has no significant difference. This is shown in the Figure 5.22. The time step size of two days gives better results and easiest calculation of the production performance parameters.

5.3.4 Effects of Steam Temperature

Steam is the only heat supplying media for cyclic steam stimulation process. The heat contained by the steam depends on the steam quality and saturation temperature of the steam. But the latent heat of steam decreases with the increase of temperature. Two

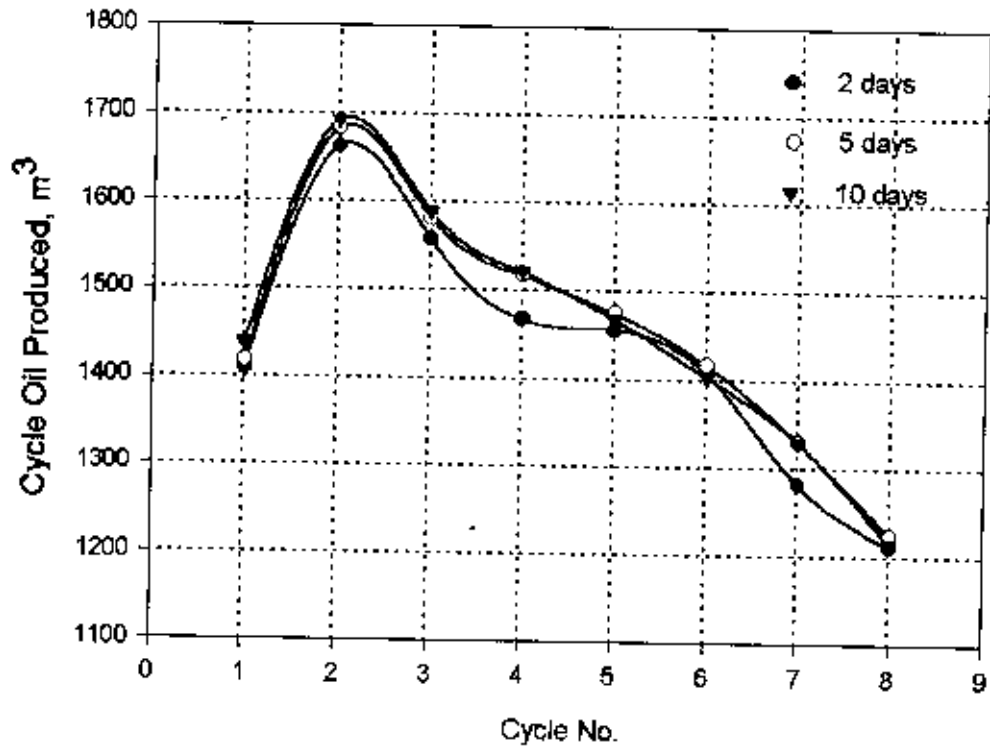


Figure 5.19- Oil production at each cycle for various production time steps.

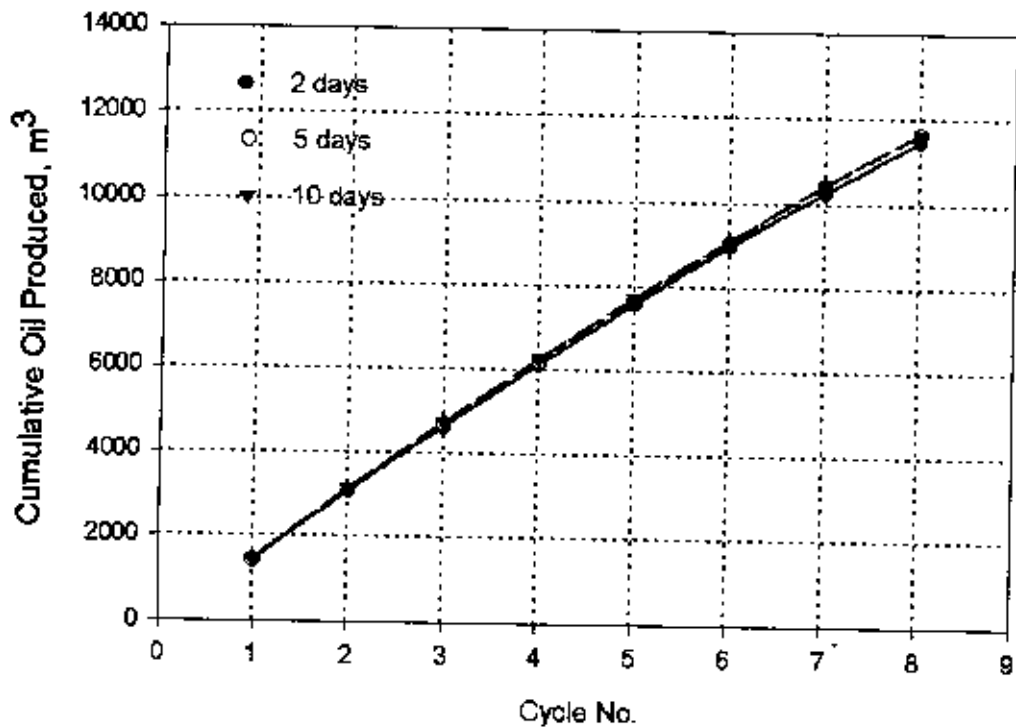


Figure 5.20- Cumulative oil production for various production time steps.

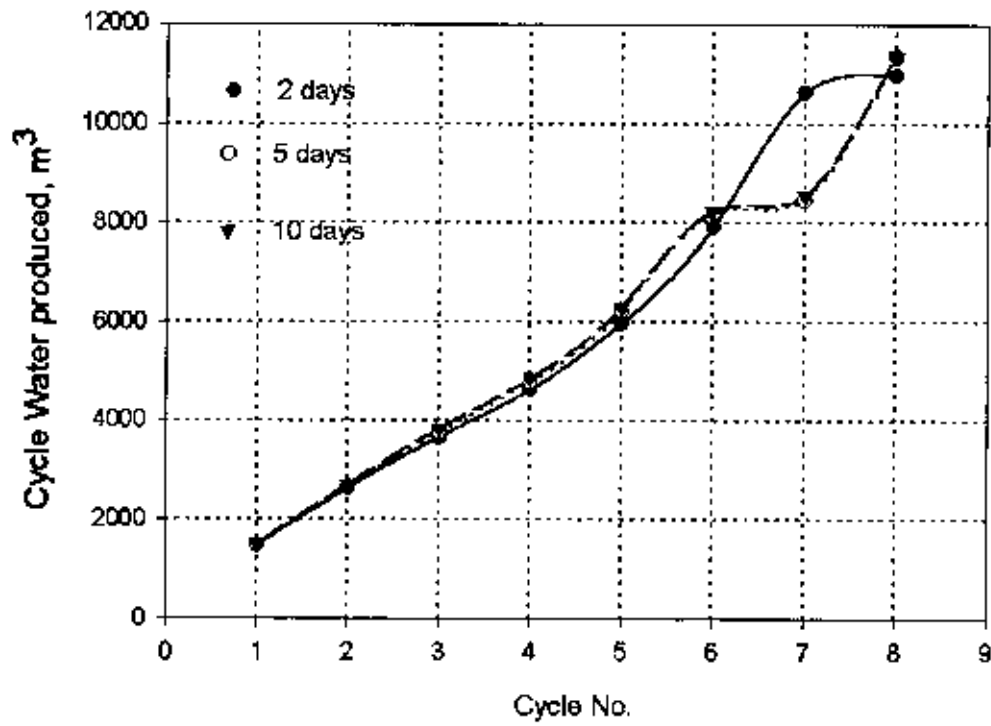


Figure 5.21- Water production at each cycle for various production time steps.

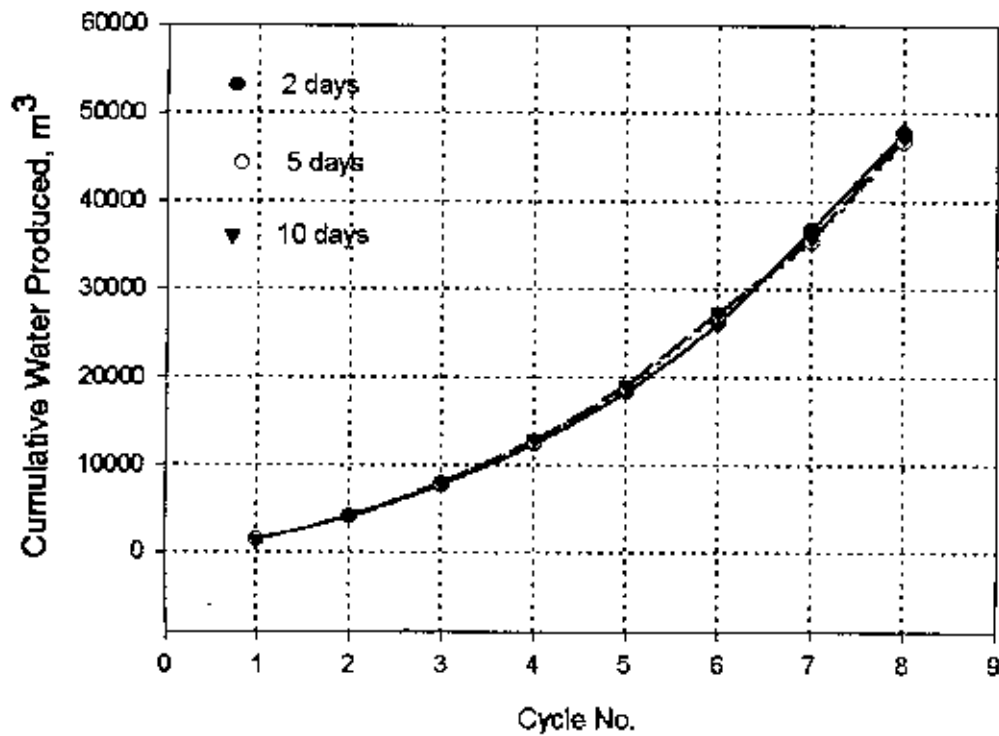


Figure 5.22- Cumulative water production for various production time steps.

steam temperatures of 50°C and 70°C above the base saturation temperature are conducted to investigate the effects of steam temperature. The quality of the steam remains unchanged. Figure 5.23 shows the cycle oil production for different steam temperatures. The higher temperature (70°C) produces more oil in the early cycles and less oil after 6th cycle compared with the base case. On the other hand the 50°C produces more oil upto the 7th cycle and decreased sharply in the next cycle. The reason could be the more heat loss occurred at higher temperature. The cumulative oil productions are shown in the Figure 5.24. Both the temperatures above base case give higher total oil production. It is seen that the 70°C produce 20% more total oil than base case. The cycle water productions are shown in the Figure 5.25. There is a little difference in cycle water production between 50°C and 70°C above base temperature setting, but it produces more cycle water than the base case. Figure 5.26 shows the total water production. It indicates that the early cycles have little difference of water production, but the latter cycles have significant difference. At the end of 8th cycle the 50°C produces 18000 m³ more water and 70°C produces 23000 m³ than the base case. The higher temperature produces approximately 40% more water than base temperature. The higher temperature setting gives better result than base case, but it increased the heat loss and also the cost of steam generation. The operational cost may not justify increasing the steam temperature.

5.3.5 Effects of Steam Quality

The amount of heat injected into the formation in CSS process depends on the steam quality at a given temperature. At higher steam quality the latent heat part of the total heat content increases. Latent heat plays a significant role in steam zone expansion. The steam qualities of 70% and 90% are conducted with the base run of 80% to investigate the effects of steam quality in CSS process. Figure 5.27 shows cycle oil production for various steam qualities. Both the high and low steam qualities produces approximately the same oil as the base case. The cumulative oil productions are shown in the Figure

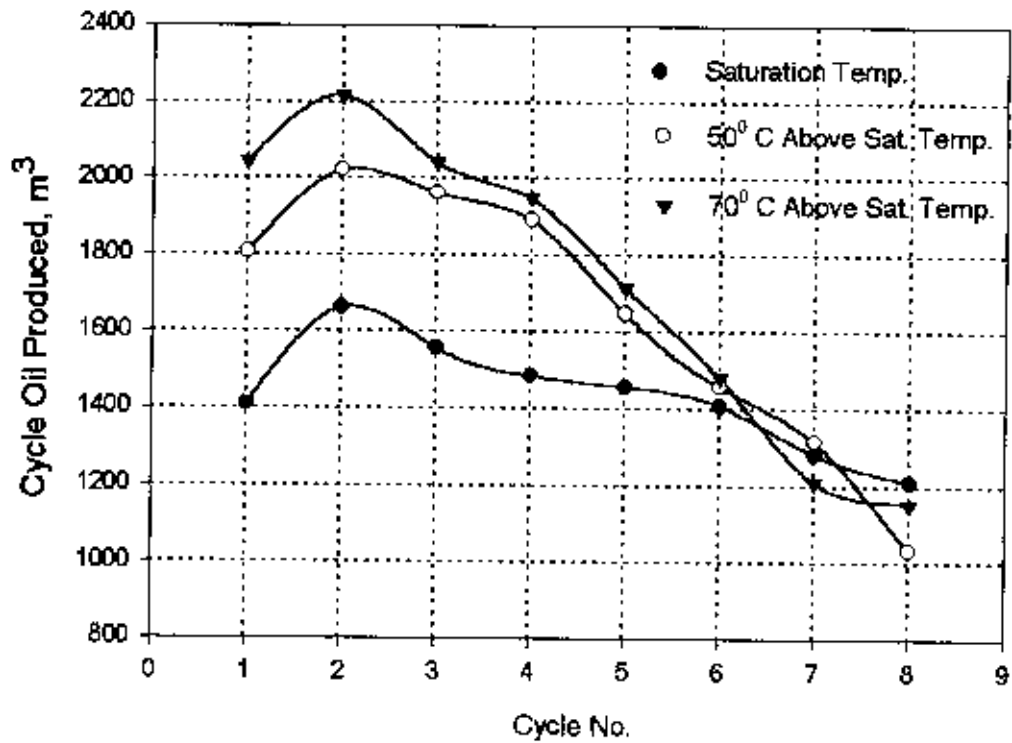


Figure 5.23- Oil production at each cycle for different steam temperatures.

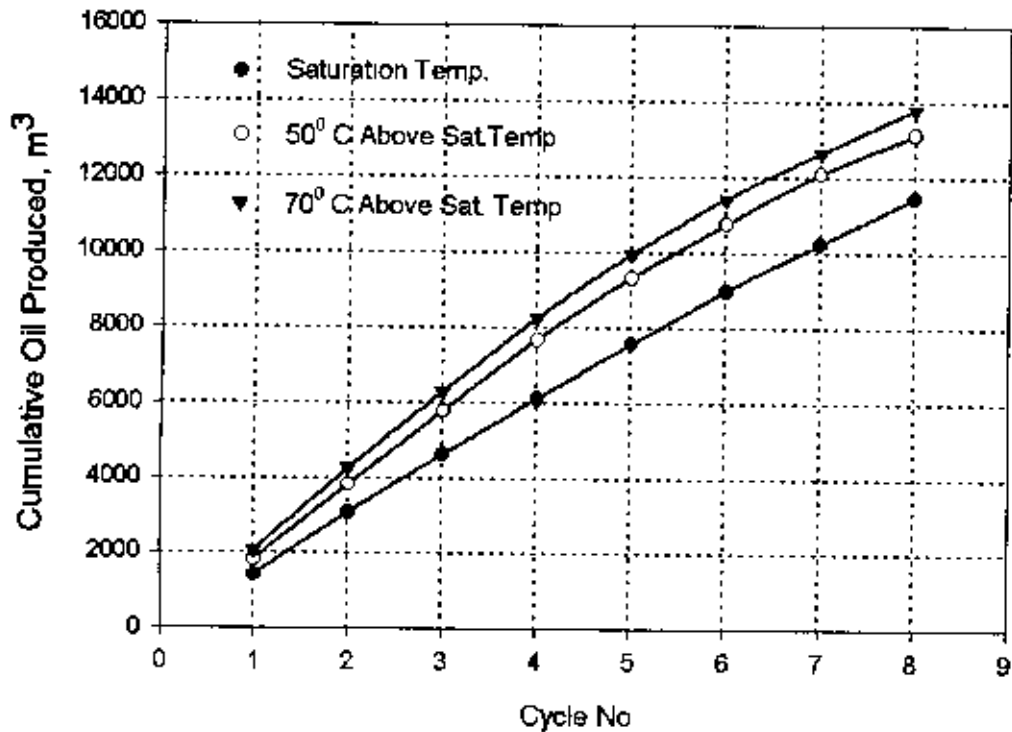


Figure 5.24- Cumulative oil produced for different steam injection temperatures.

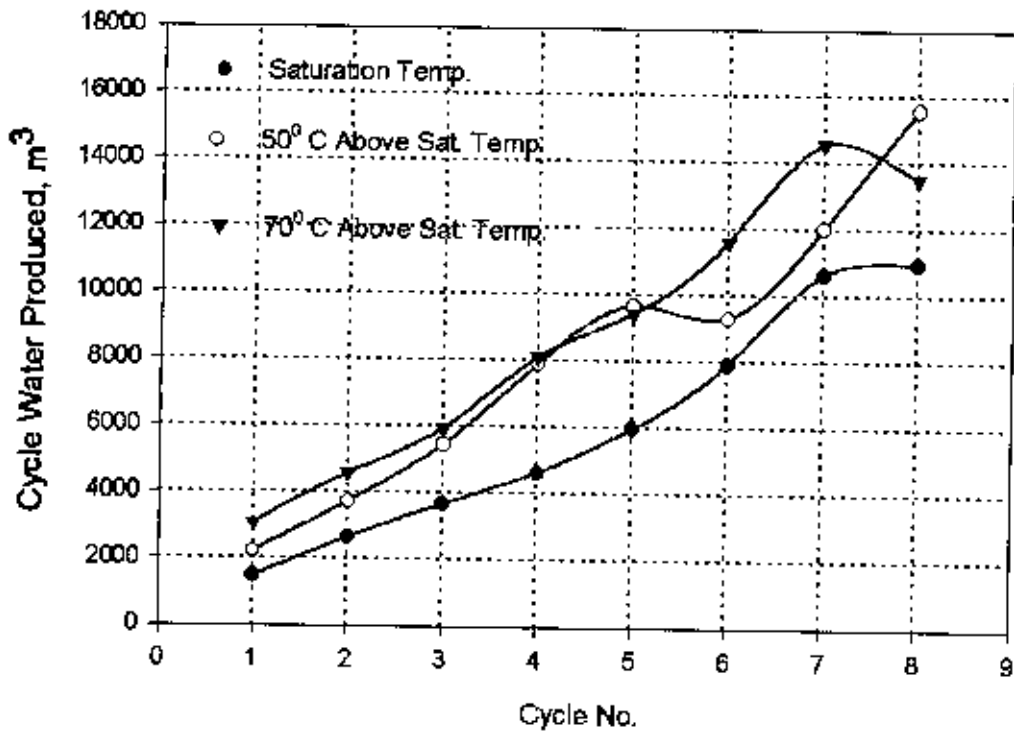


Figure 5.25- Water production at each cycle for various steam injection temperatures.

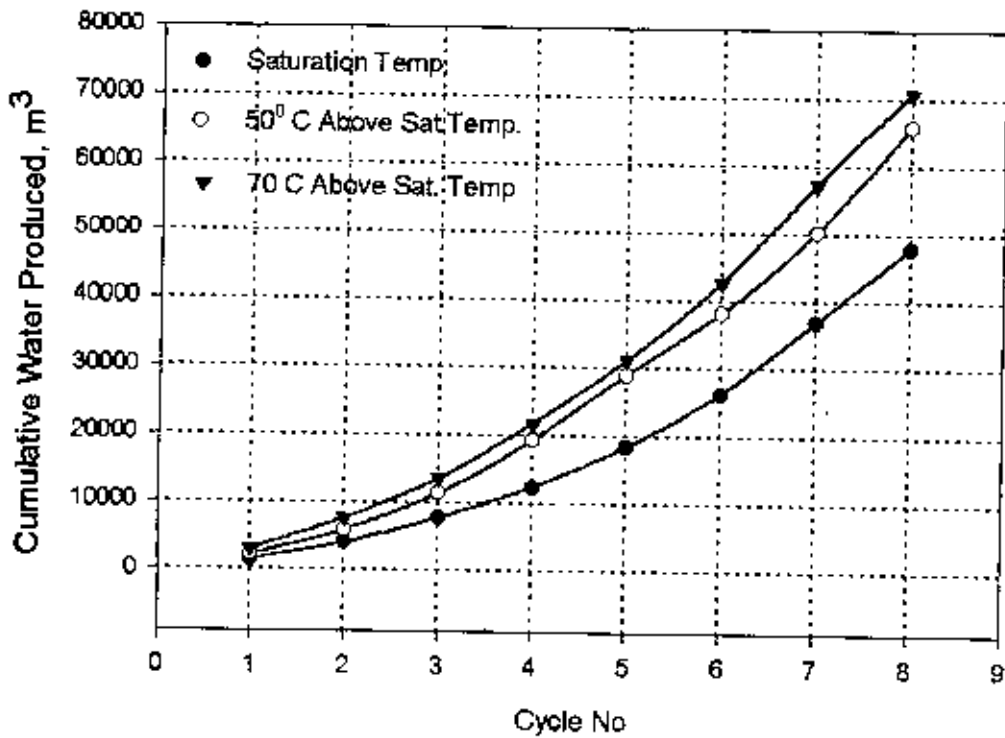


Figure 5.26- Cumulative water produced for different steam injection temperatures.

5.28. It indicates that the same total oil is produced for all three cases. It is seen that increasing steam qualities produces marginally higher oil. The reason is the increase of average reservoir temperature with the increase of steam quality. Figure 5.29 shows the cycle water production for various steam qualities. Early cycles produce approximately the same water, but the later cycles produce little more water with increasing steam quality. The total water productions are shown in the Figure 5.30. The appreciable amount of difference appears after 5th cycle for different steam qualities. At the end of 8th cycle the 70% quality of steam produces 46661 m³ water and 90% quality produces 48862 m³ water. Whereas base run of 80% quality produces 47873 m³ water. The reason may be the increase of slug size in the later cycle. So the setting of steam quality for this model can vary from 70% to 90%. Wellhead steam qualities of 70% to 85% are most widely produced in the field. This range of steam quality gives ultimate better production performance.

5.3.6 Effects of Formation Thickness

The formation thickness affects the oil production rate from heavy oil reservoirs during cyclic steam stimulation process. The net pay thickness of 20 m and 30 m are investigated along with the base run thickness 23.8 m. Figure 5.31 shows the cycle oil production for different pay thickness. The higher pay thickness produces more oil in early cycles and decreases in the later cycles compared with the base case. Whereas lower pay thickness produces always less oil than the base case. The total oil productions for different pay thickness are shown in the Figure 5.32. It indicates that uniform difference exists in all the cycle for different pay thickness. It is said that higher pay thickness occupy the more drainage area of the reservoir and produces more oil in the early cycle but the oil production decreases in later cycle due to the constant volume of injected steam. Figure 5.33 shows the cycle water production for different pay thickness. The higher pay thickness always produces more water than the base case. Whereas lower pay thickness produces much less water in later cycles than the

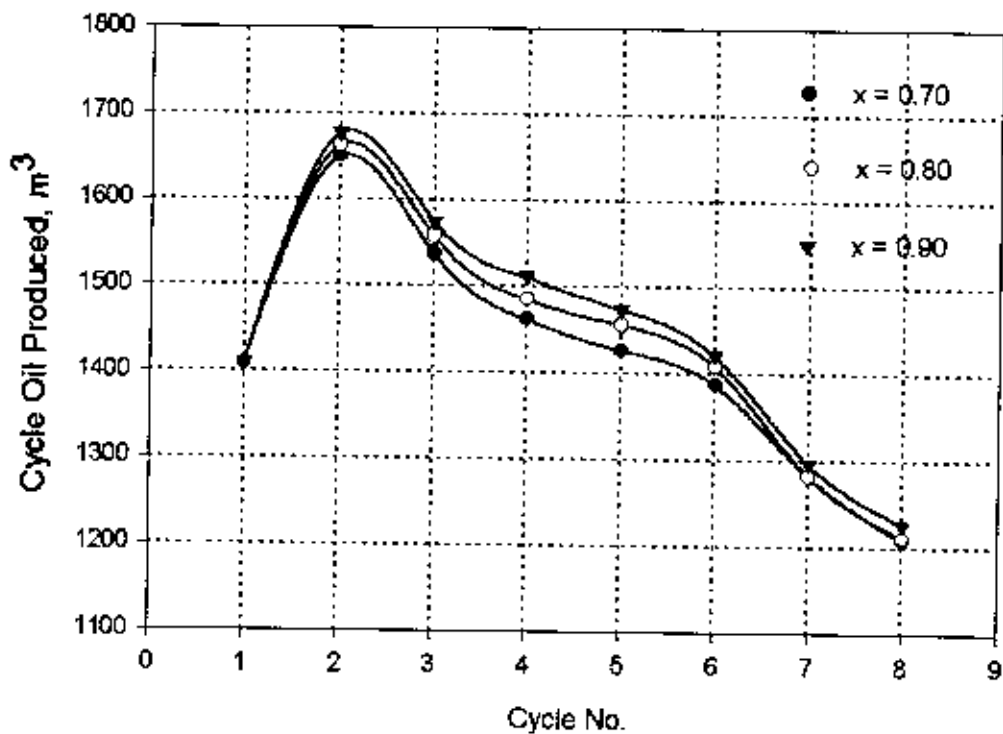


Figure 5.27- Oil production at each cycle for various steam qualities.

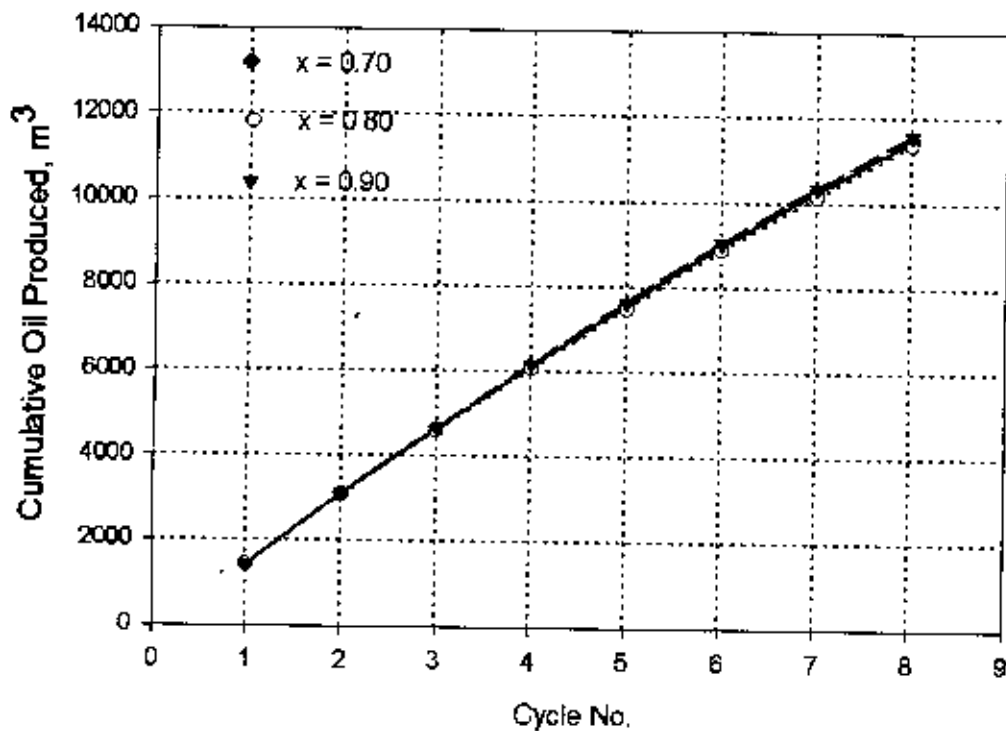


Figure 5.28- Cumulative oil produced for various steam qualities.

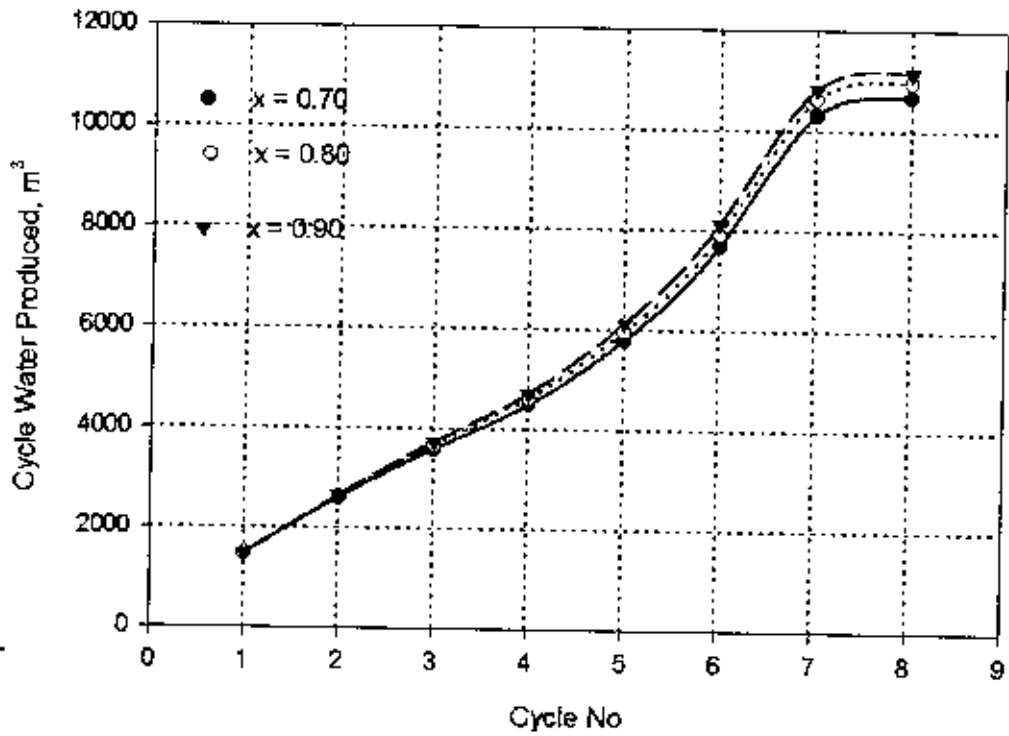


Figure 5.29- Water production at each cycle for various steam qualities.

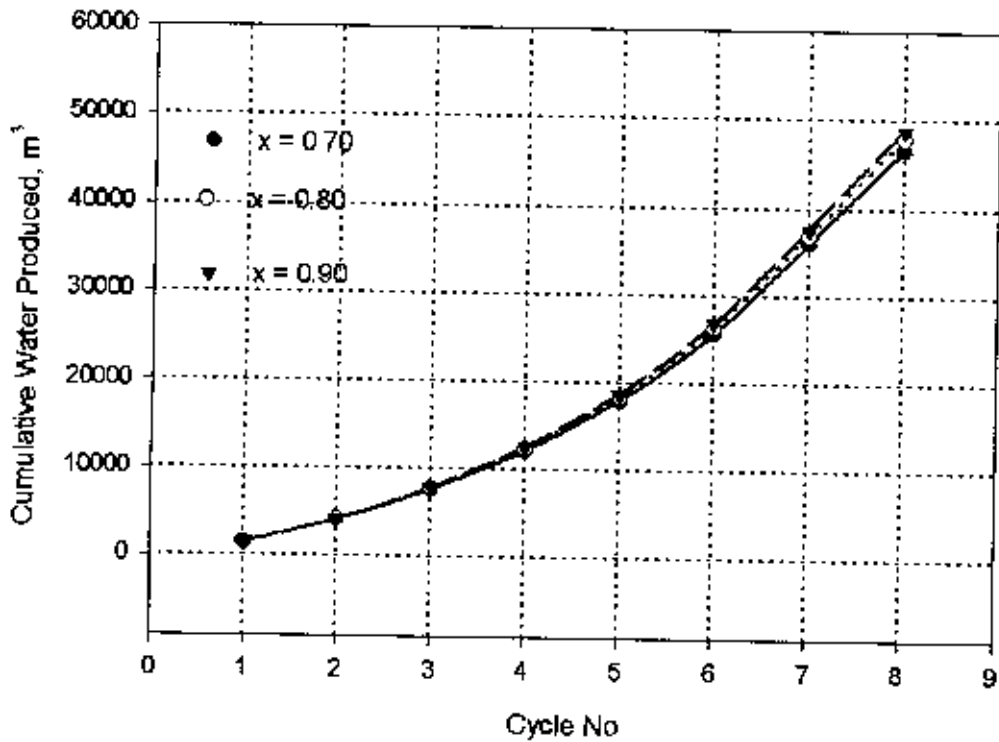


Figure 5.30- Cumulative water production for various steam qualities.

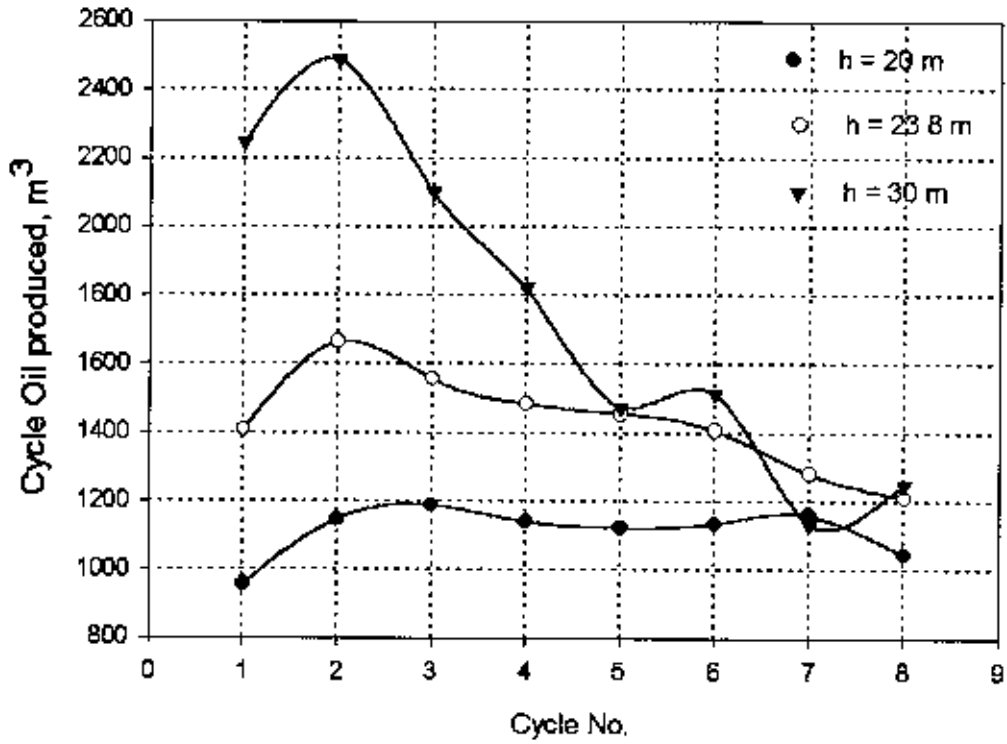


Figure 5.31- Oil produced at each cycle for different pay thickness.

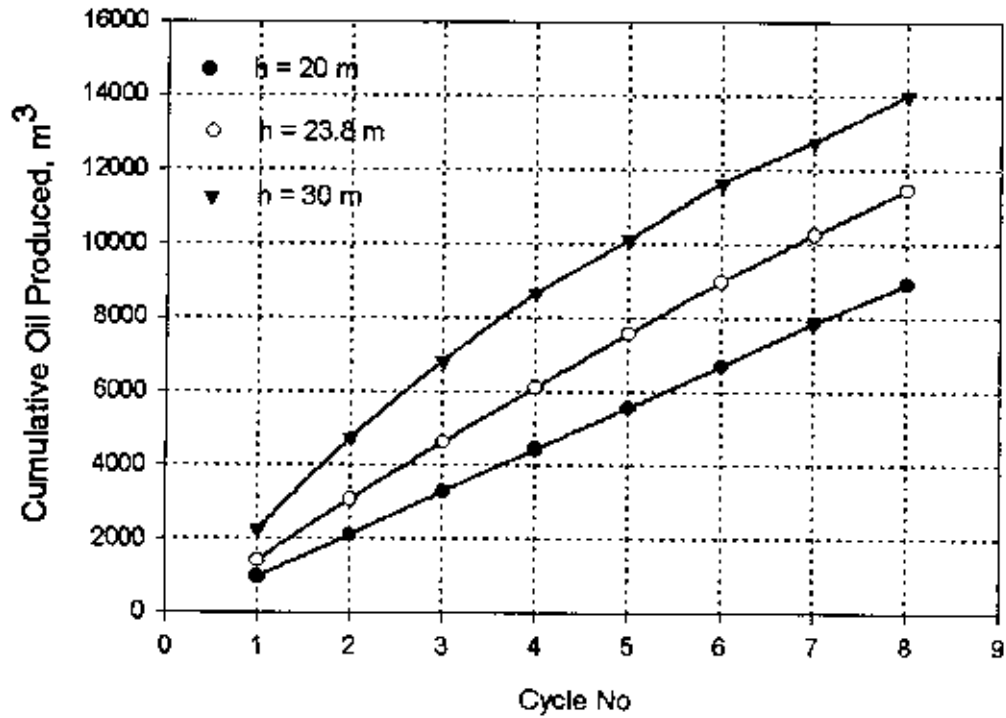


Figure 5.32- Cumulative oil production for different pay thickness.

91810

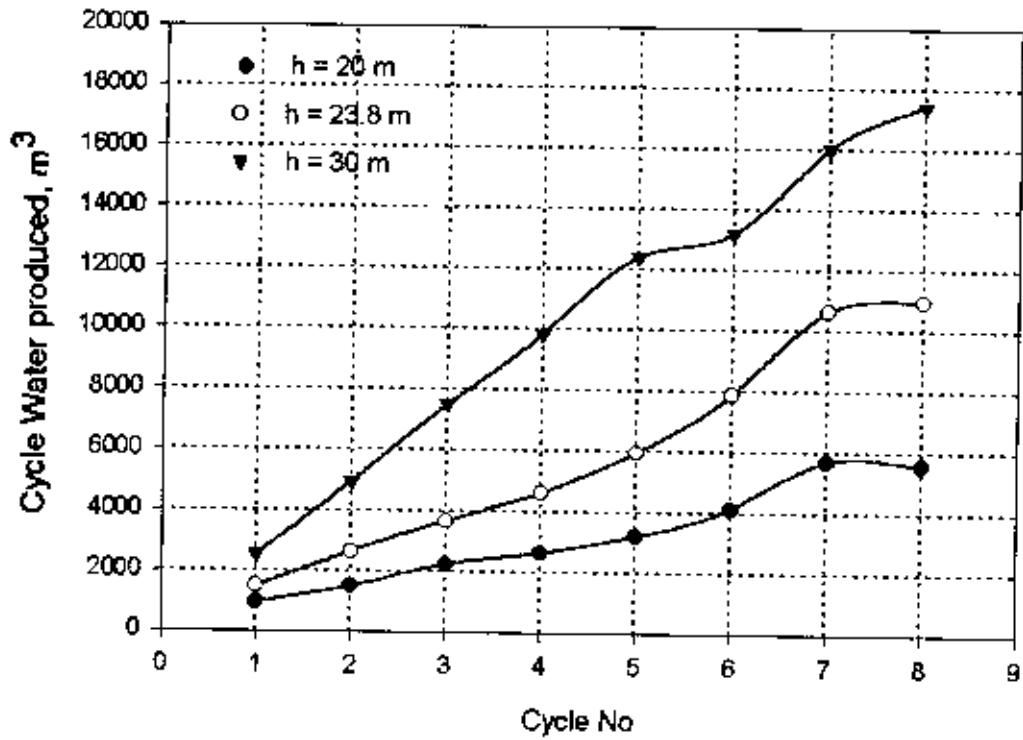


Figure 5.33- Water produced at each cycle for different pay thickness.

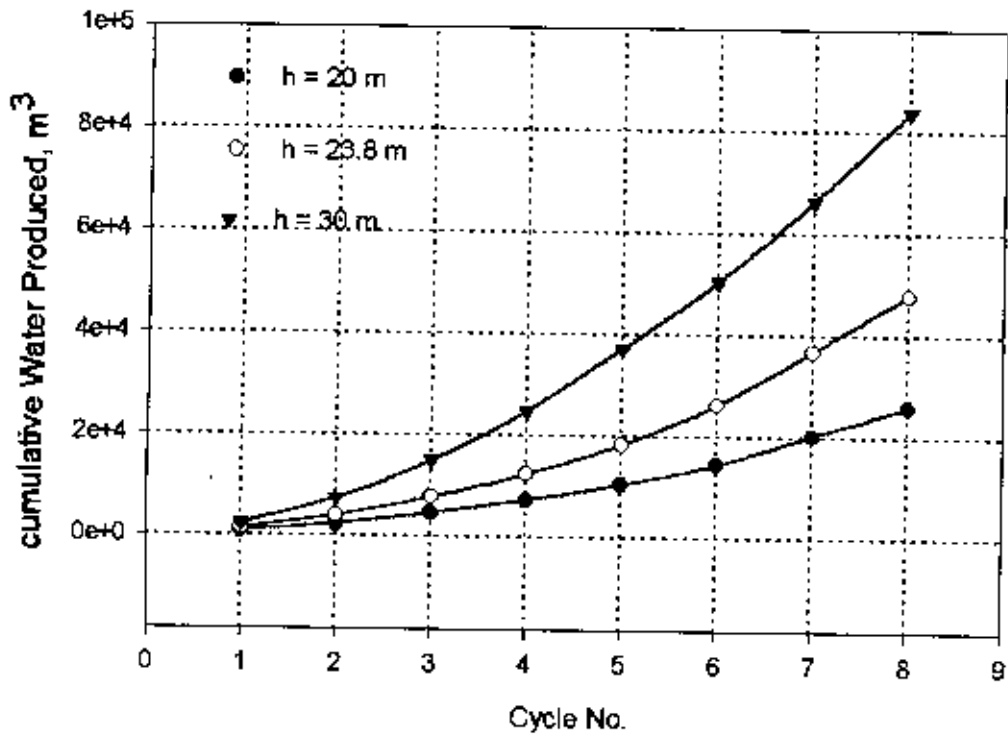


Figure 5.34- cumulative water production for different pay thickness.

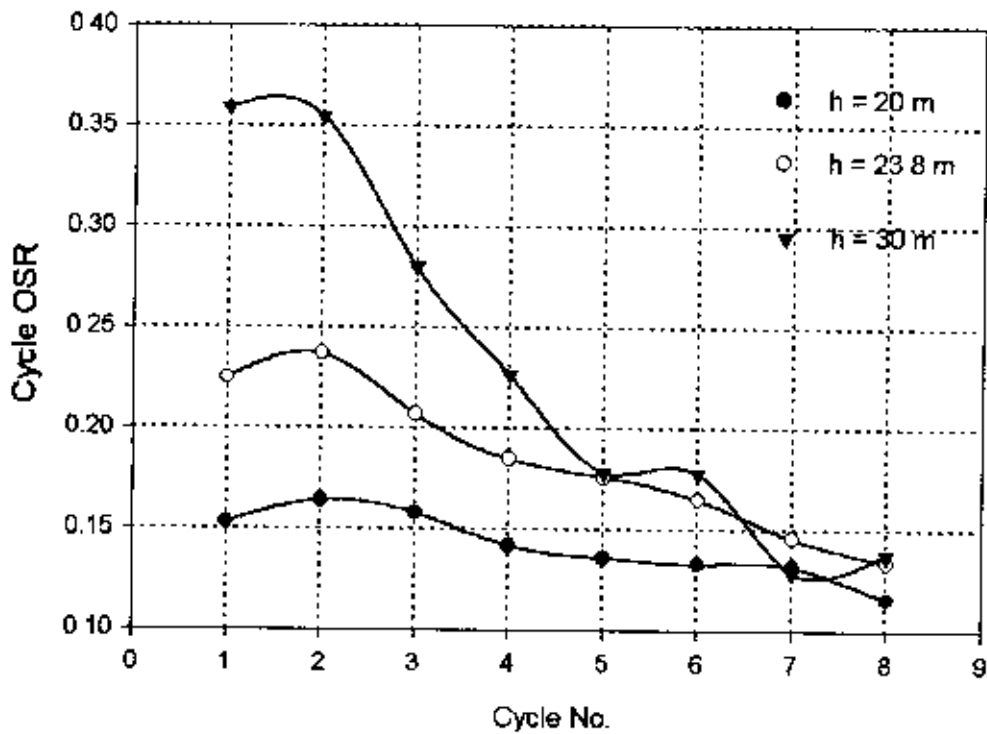


Figure 5.35- Oil-Steam ratio at each cycle for various pay thickness.

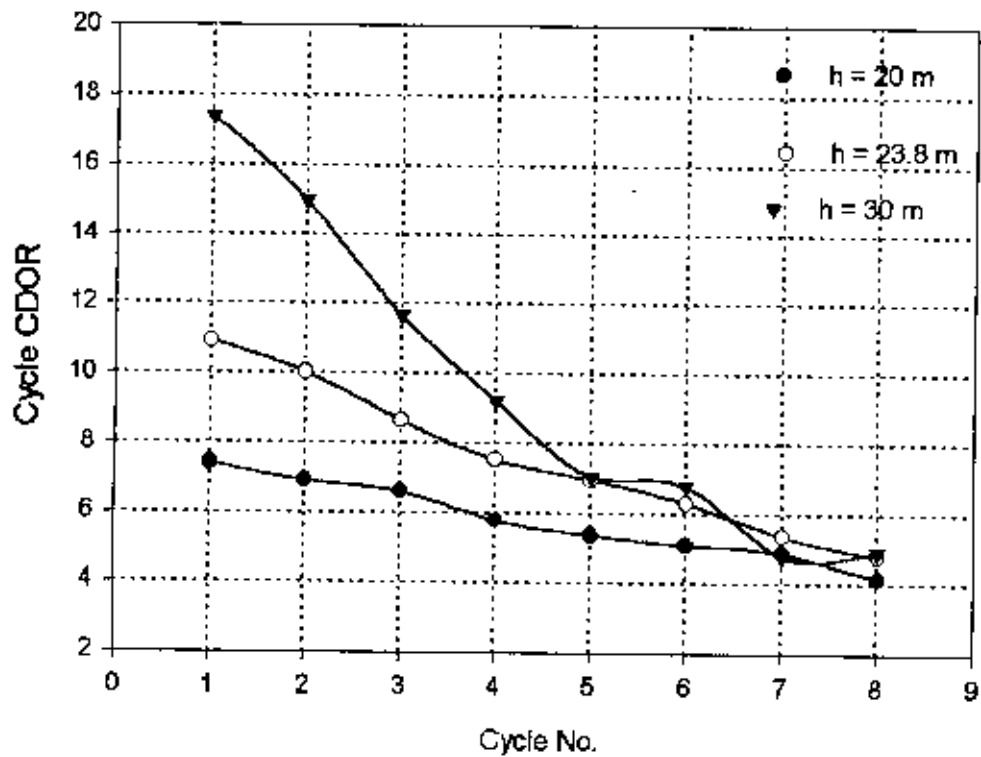


Figure 5.36 - Calendar day oil production rate at each cycle for different pay thickness.

early cycles compared with the base case. The total water productions for different pay thickness are shown in the Figure 5.34. Early cycles produces less difference for water production, but later cycles have higher difference. At the end of 8th cycle the 20 m pay thickness produces 25950 m³ of water and 30 m produces 83834 m³ of water compared with base the case produces 47873 m³ of water. Figure 5.35 shows the oil-steam ratio at each cycle for various pay thickness. The higher pay thickness produces more oil-steam ratio upto 5th cycle and then decreases compared with base run pay thickness 23.8m. Whereas lower pay thickness always produces less OSR than base case. The actual reason could not be understood. The calendar day oil production rate(CDOR) shows the same trend as OSR curve. This is shown in Figure 5.36. The reason may be higher the pay thickness, lesser the heat loss to the over and underburden. So the net pay thickness significantly affects the performance parameter.

CONCLUSIONS AND RECOMMENDATIONS

An analytical model has been developed in this study to predict production performance of heavy oil reservoirs undergoing cyclic steam stimulation process. After successfully matching a previously reported field data and an extensive sensitivity analysis, the following conclusions are reached as follows.

1. The model has been developed for elliptical flow geometry with a circular wellbore at the center of an ellipse.
2. The fractures and microchannels created during steam injection remains open or partially open during production period depending on the pressure of the reservoir. This condition increases the reservoir permeability and porosity which practically enhances the flow rate.
3. For the first time, the shear failure zone of heavy oil reservoir has been simulated by means of pseudo-relative permeability functions in an analytical model.
4. An extensive sensitivity study has been done by using the various reservoir and steam properties. The model responded in a reasonable and acceptable manner for all the imposed variation in the properties. It was found that the model is applicable over a wide variety of reservoir and operating conditions.
5. The predicted results successfully match with field results upto the sixth cycle. The model has limited utility beyond the sixth cycle.

6. This model can be successfully used as a valuable tool for operational control. This can also be used for quick assessment and analysis prior to an expensive numerical simulation.

Recommendations

During the course of this study, various ideas to improve the model could not be accommodated due to time constraints and limited scope of the present study. Some of these ideas are presented here for future improvement of the model and the study.

1. To investigate the shear stress in the failure zone.
2. To accommodate the direction of fractures and microchannels.
3. To check the model with more field data.
4. To investigate the porosity change in the failure zone.

REFERENCES

- Arthur, J.E., Best, D.A., Jha, K.N. and Mourits, F.M. (1991): "An Analytical Composite Model for Cyclic Steam Stimulation in Elliptical Flow Geometry," presented at the 5th UNITAR Conference on Heavy Crude and Tar sands, Caracas, Venezuela, Aug. 4-9.
- Bang, H.W. (1984): "Simulation Study Shows hysteresis Effect on Oil Recovery During a Cyclic Steam Process," *Oil and Gas J.* (Feb.) 83-86.
- Barker, J.W. and Thibeau, S. (1997): "A Critical Review of the Use of Pseudorelative Permeabilities for Upscaling," *SPE* (May) 138-143.
- Beattie, C.L., Boberg, T.C. and McMab, G.S. (1991): "Reservoir Simulation of Cyclic Steam Stimulation in the Cold Lake Oil Sands," *SPE* (May) 200-206.
- Beier, R.A. (1994): "Pseudo-relative Permeabilities from Fractal Distributions," *SPE Advanced Technology Series* (April) 132-139.
- Boberg, T.C. and Lantz, R.B. (1966): "Calculation of the Production Rate of a Thermally Stimulated Well," *JPT* (December) 1613-1623.
- Boone, T.J., Gallant, R.J. and Kry, P.R. (1993): "Exploiting High-Rate Injection and Fracturing To Improve Areal Thermal Conformance in Cyclic Steam Stimulation," SPE 25796, presented at the International Thermal Operations Symposium, Bakersfield, CA, USA, Feb. 8-10.

Bulter, R.M., McNab, G.S. and Lo, H.Y. (1979): "Theoretical Studies on the Gravity Drainage of Heavy Oil During In-Situ Steam Heating," presented at the 29th Canadian Chemical Engineering Conference, Sarina, ON, October 1-3.

Carslaw, H.S. and Jaeger, T.C. (1965): *Conduction of Heat in Solids*, Oxford Press, London, 58-61.

Carter, R.D. (1957): "Derivation of The General Equation for Estimating the Extent of Fracture Area," Appendix to: "Optimum Fluid Characteristics for Fracture Extension," by Howard, G.C. and Fast, C.R., *Drilling and Production Prac.*, (April) 261-270.

Chen, H.L. and Sylvester, N.D. (1990): "Appraisal of Analytical Steamflood Models," SPE 20023, presented at the 60th California Regional Meeting of the SPE, ventura, CA, April 4-6.

Davidson, L.B., Miller, F.G. and Mueller, T.D. (1967): "A Mathematical Model of Reservoir Response During the Cyclic Injection of Steam," *SPEJ* (June) 174-188.

Denbina, E.S., Boberg, T.C. and Rotter, M.B. (1991): "Evaluation of Key Reservoir Drive Mechanism in the Early Cycles of Steam Stimulation at Cold Lake," *SPEE* (May) 207-211.

Dietrich, J.K. (1981): "Relative Permeability During Cyclic Steam Stimulation of Heavy Oil," *JPT* (October) 1987-1989.

Dietrich, J.K. (1986): "Cyclic Steaming of Tar Sands Through Hydraulically Induced Fracture," *SPEE* (May) 217-229.

Ekram, S. And Mykkeltveit, J. (1995): "Dynamic Pseudos: How Accurate Outside Their Parent Case?," SPE 29138, presented at the 13th SPE Symposium on Reservoir Simulation, San Antonio, TX, February 12-15.

Farouq Ali, S.M. (1982): "Steam Injection Theories - A Unified Approach," SPE 10746, presented at the California Regional Meeting of the SPE, San Francisco, CA, March 24-26.

Gajdica, R.J., Brigham, W.E., and Aziz, K. (1990): "A Semi-analytical Thermal Model for Linear Steam Drive," SPE 20198, presented at the Seventh Symposium on Enhanced Oil Recovery of SPE, Tulsa, April 22-25.

Gontijo, J.E. and Aziz, K. (1984): "A Simple Analytical Model for Simulating Heavy Oil Recovery by Cyclic Steam in Pressure Depleted Reservoirs," SPE 13037, presented at the 59th Annual Technical Conference and Exhibition, Houston, TX, September 16-19.

Gozde, S., Chhina, H.S. and Best, D.A. (1989): "An Analytical Cyclic Steam Stimulation Model for Heavy Oil Reservoirs," SPE 4757, Presented at the California Regional Meeting of SPE, Bakersfield, CA, April 5-7.

Gringarten, A.C., Ramey, J.R. and Raghavan, R. (1974): "Unsteady-State Pressure Distributions Created by a Well With a Single Infinite-Conductivity Vertical Fracture," SPEJ (August) 347-360.

Hearn, C.L. (1971): "Simulation of Stratified Waterflooding by pseudo Relative Permeability Curves," SPE 2929 (July) 805-813.

Hong, K.C. (1994): "Effects of Steam Quality and Injection Rate on Steamflood Performance," SPERE (September) 53-64.

Ito, Y. (1984): "The Introduction of the Microchanneling Phenomenon to Cyclic Steam Stimulation and Its Application to the Numerical Simulator (Sand Deformation Concept)," SPE (August) 417-429.

Ito, Y., Settari, A., Kry, P.R. and Jha, K.N. (1993): "Development and Application of Pseudo-Functions for Reservoir Simulation To Represent Shear Failure During the Cyclic Steam Process," presented at the Thermal Operation Symposium in Bakersfield, CA, February 8-10.

Ito, Y., Settari, A. and Jha, K. (1993): "The Effects of shear Failure on the Cyclic Steam Process and New Pseudo Functions for Reservoir Simulation," JCPT (December) 39-48.

Jacks, H.H., Smith, O.J.E. and Mattax, C.C. (1972): "The Modeling of a Three-Dimensional Reservoir with a Two-Dimensional Reservoir Simulator-The Use of Dynamic Pseudo Functions," SPE 4071, presented at the SPE-AIME 47th Annual Fall Meeting, San Antonio, Tex., October 8-11.

Jones, J. (1977): "Cyclic Steam Reservoir Model for Viscous Oil, Pressure Depleted, Gravity Drainage Reservoirs," SPE 6544, presented at the California Regional Meeting of SPE, Bakersfield, April 13-15.

Kucuk, F. and Brigham, W.E. (1981): "Unsteady-State Water Influx in Elliptical and Anisotropic Reservoir/Aquifer Systems," SPEJ (June) 119-126.

Marx, J.W. and Langenheim, R.H. (1956): "Reservoir Heating by Hot Fluid Injection," Trans., AIME, 216, 312-315.

McGee, B.C.W., Arthur, J.E. and Best D.A. (1987): "Analytical Analysis of Cyclic Steam Stimulation Through Vertical Fractures," presented at the 38th Annual Technical Meeting of CIM, Calgary, AB, June 7-10.

Muskat, M. (1937): *Flow of Homogeneous Fluids*, McGraw-Hill Book Company Inc., New York, 191, 389.

Nakornthap, K. and Evans, R.D. (1986): "Temperature-Dependent Relative Permeability and Its Effect on Oil Displacement by Thermal Methods," *SPE* (May) 230-242.

Owens, W.D. and Suter, V.E. (1965): "Steam Stimulation for Secondary Recovery," *JCPT* (Oct.- Dec.) 227-235.

Peake, W.T. (1984): "Reservoir Simulation of Steam Injection in the Cold Lake Tar Sand," *SPE* 13038, presented at the 59th Annual Technical Conference and Exhibition, Houston, Texas, September 16-19.

Pethrick, W.D. Sennhauser, E.S. and Harding, T.G. (1988): "Numerical Modeling of Cyclic Steam Stimulation in Cold Lake Oil Sands," *JCPT* (Nov.-Dec.) 89-97.

Powers, W.L., Kirkham, D. and Snowden, G. (1967): "Orthonormal Functions Tables and the Seepage of steady Rain through Soil Bedding," *J. of Geophysical Research*, 72(24) 6225-6237.

Prats, M., Hazebroek, P. And Strickler, W.R. (1962): "Effect of Vertical Fracture on Reservoir Behavior- Compressible Fluid Case," *SPEJ* (June) 87-94.

Saad, N., Cullick, A.S. and Honarpour, M.M. (1995): "Effective Relative Permeability in Scale-Up and Simulation," SPE 29592, presented at the SPE Rocky Mountain Regional/Low-Permeability Reservoirs Symposium, Denver, CO, March 20-22.

Settari, A. and Raisbeck, J.M. (1981): "Analysis and Numerical Modeling of Hydraulic Fracturing During Cyclic Steam Stimulation in Oil Sands," SPE 9087, (November) 2201-2212.

Settari, A. (1989): "Physics and Modeling of Thermal Flow and Soil Mechanics in Unconsolidated Porous Media," SPE 18420, presented at the SPE symposium on Reservoir Simulation, Houston, TX, February 6-8.

Smith-Magowan, D., Skauge, A. And Hepler, L.G. (1982): "Specific Heat of Athabasca Oil Sands and Components," JCPT (May-June) 28-32.

Stanislav, J.F., Easwaran, C.V. and Kokal, S.L. (1987): "Analytical Solutions for Vertical Fractures in a Composite System," JCPT (Sept.-Oct.) 51-56.

Stone, H.L. (1991): "Rigorous Black Oil Pseudo Functions" SPE 21207, presented at the 11th SPE Symposium on Reservoir Simulation, Anaheim, CA, February 17-20.

Sylvester, N.B. and Chen, H.L. (1988): "An Improved Cyclic Steam Stimulation Model for Pressure-Depleted Reservoirs," SPE 17420, presented at the California Regional Meeting of SPE, Long Beach, March 23-25.

Tarnim, M. and Farouq Ali, S.M. (1995): "A New Analytical Cyclic Steam Stimulation Model Including Formation Fracturing," The Petroleum Society of CIM, Alberta, Canada, Paper 95-61, May 14-17.

Tuefel, L.W. and Rhett, D.W. (1991): "Geomechanical Evidence for Shear Failure of Chalk During Production of the Ekofisk Field," SPE 22755, presented at the 66th Annual Technical Conference and Exhibition of the SPE, Dallas, TX, October 6-9.

Van Everdingen, A.F. and Hurst, W. (1949): "The Application of Laplace Transformation to Flow Problems in Reservoirs," Trans., AIME, 186, 305-324.

van der Ploeg, R.R., Kirkham, D. and Boast, C.W. (1971): "Steady State Well Flow Theory for a Confined Elliptical Aquifer," Water Resources Research (August) 942-954.

Van Wunnik, J.N.M. and Wil, K. (1992): "Improvement of Gravity Drainage by Steam Injection into a Fractured Reservoir: An Analytical Evaluation," SPERE (February) 59-66.

Vinsome, P.K.W. and Westerveld, J. (1980): "A Simplified Method for Predicting Cap and Base Rock Heat Losses in Thermal Reservoir Simulators," JCPT (July-Sept.) 87-90.

Vogel, J.V. (1984): "Simplified Heat Calculations for Steam Drive," JCPT (July) 1127-1136.

Wheeler, J.A. (1969): "Analytical Calculations for Heat Transfer from Fractures," SPE 2494, Improved Oil Recovery Symposium of SPE, Tulsa, April 13-15.

APPENDIX A

FLOW INTO A WELL LOCATED AT THE CENTER OF AN ELLIPTICAL DRAINAGE BOUNDARY (Tamim, 1995)

The fluid flow from heated reservoirs into the wellbore is elliptic. Ploeg, Kirkham and Boast (1971) presented a solution for steady saturated flow in an elliptical confined aquifer. They considered the aquifer to be isotropic and homogeneous. They developed potential and stream functions for a number of different shaped aquifer and well locations. The variety of geometries are considered enables to predict the well discharge for aquifers that approach the shape of an ellipse.

A.1 Well at the center of an ellipse

By considering an elliptical aquifer with the well located in the center. The equation in rectangular co-ordinates of an ellipse is

$$\frac{x^2}{a^2} + \frac{y^2}{b^2} = 1 \quad (\text{A.1})$$

Using polar co-ordinates (R, θ)

$$x = R \cos\theta, \text{ and } y = R \sin\theta$$

The equation (A.1) can be written in the following form

$$R^2 \left(\frac{\cos^2 \theta}{a^2} + \frac{\sin^2 \theta}{b^2} \right) = 1. \quad (\text{A.2})$$

A.1.1 Boundary conditions

$$\text{B.C 1: } \Phi = 0 \quad \text{for } r = r_w \quad 0 \leq \theta \leq \pi/2$$

$$\text{B.C 2: } \Phi = 1 \quad \text{for } r = R \quad 0 \leq \theta \leq \pi/2$$

$$\text{B.C 3: } \partial\Phi/\partial\theta = 0 \quad \text{for } \theta = 0 \quad r_w < r < a$$

$$\text{B.C 4: } \partial\Phi/\partial\theta = 0 \quad \text{for } \theta = \pi/2 \quad r_w < r < b$$

The Laplace equation in polar co-ordinates gives an expression for the hydraulic head Φ ,

$$\frac{\partial^2 \Phi}{\partial r^2} + \frac{1}{r} \frac{\partial \Phi}{\partial r} + \frac{1}{r^2} \frac{\partial^2 \Phi}{\partial \theta^2} = 0 \quad (\text{A.3})$$

A.1.2 Solution of Laplace Equation

The solution of equation (A.3) by using the Gram-Schmidt method gives the following expression for hydraulic head,

$$\Phi = \sum_{m=0}^N A_m u_m(r, \theta) \quad (\text{A.4})$$

where, $m = 0, 1, 2, \dots, N$;

$N = 0, 1, 2, \dots, \infty$;

$$\text{and } u_m(r, \theta) = \frac{\left(\frac{r}{a}\right)^{2m} - \left[\frac{r_w^2}{(ar)}\right]^{2m}}{1 - \left(\frac{r_w^2}{a^2}\right)} \cos 2m\theta. \quad (\text{A.5})$$

On the boundary of the ellipse $r = R$ and using equation (A.2) for express R in terms of θ . The equation (A.5) becomes,

$$u_m(\theta) = \frac{\left(\frac{R^2}{a^2}\right)^m - \left[\frac{r_w^2}{a^2} \frac{r_w^2}{R^2}\right]^m}{1 - \left(\frac{r_w^2}{a^2}\right)^{2m}} \cos 2m\theta, \quad (\text{A.6})$$

Now the equation for hydraulic head,

$$\Phi_{r=R} = \sum_{m=0}^N A_{Nm} u_m(\theta), \quad 0 \leq \theta \leq \pi/2 \quad (\text{A.7})$$

To satisfy the boundary condition B.C. 2, the equation (A.7) in the following form,

$$I = \sum_{m=0}^N A_{Nm} u_m(\theta), \quad 0 \leq \theta \leq \pi/2 \quad (\text{A.8})$$

Powers et al. (1967) determine the value of A_{Nm} by using an orthonormal function table. They introduce two constants w_m and u_{mn} are,

$$w_m = \int_0^{\pi/2} (1) u_m(\theta) d\theta, \quad m = 0, 1, 2, \dots, N \quad (\text{A.9})$$

$$u_{mn} = \int_0^{\pi/2} u_m(\theta) u_n(\theta) d\theta, \quad m = 0, 1, 2, \dots, N \quad m \geq n \quad (\text{A.10})$$

where the $u_m(\theta)$ and $u_n(\theta)$ are obtained from equation (A.6)

The solution of the above integrations are difficult in analytical method. For accurate solution, numerical integration method is used. The Gaussian quadrature method gives the best solution of w_m and u_{mn} . Terms with zero subscript produced by using L'Hospital rule.

$$u_0(\theta) = \frac{\ln\left(\frac{r}{r_w}\right)}{\ln\left(\frac{a}{r_w}\right)}. \quad (\text{A.11})$$

The hydraulic head becomes,

$$\Phi = A_{N0} \frac{\ln\left(\frac{r}{r_w}\right)}{\ln\left(\frac{a}{r_w}\right)} + \sum_{m=1}^N A_{Nm} \frac{\left(\frac{r}{a}\right)^{2m} - \left[\frac{r_w^2}{ar}\right]^{2m}}{1 - \left(\frac{r_w^2}{a^2}\right)} \cos 2m\theta. \quad (\text{A.12})$$

By using the Table of Powers et al. (1967) the values of A_{Nm} are determined. Then the values of hydraulic head are determined by using equation (A.12).

A.2 Development of Formulas of Orthonormal Functions

Power, Kirkham and Snowden (1967) developed a set of general orthonormal functions for solving potential flow problems. The equation for potential function is

$$\Phi = \sum_{m=0}^{N \rightarrow \infty} A_{Nm} u_m(x) \quad (\text{A.13})$$

The above equation may be written for basic series development as

$$f(x) = \sum_{m=0}^{N \rightarrow \infty} A_{Nm} u_m(x) \quad \alpha < x < \beta \quad m = 0, 1, \dots, N \quad (N \rightarrow \infty) \quad (\text{A.14})$$

If $f(x)$ and $u_m(x)$ are known, the A_{Nm} can be determined by an auxiliary equation

$$f(x) = \sum_{m=0}^{N \rightarrow \infty} B_m \lambda_m(x) \quad (\text{A.15})$$

where B_m are constant and $\lambda_m(x)$ are an orthonormal polynomial developed from linear combination of the known $u_m(x)$.

When polynomials $\lambda_m(x)$ are orthonormal, then it can be used to developed other functions $f(x)$ into the series of the form,

$$f(x) = \sum_{m=0}^{N \rightarrow \infty} B_m \lambda_m \quad (\text{A.16})$$

where

$$B_m = \int_{\beta}^{\alpha} f(x) \lambda_m dx \quad \alpha \leq x \leq \beta \quad m = 0, 1, \dots, N \rightarrow \infty \quad (\text{A.17})$$

For each of the orthonormal polynomials an orthogonal function γ_m and a normalization factor D_m can be correlate as

$$\lambda_m = \gamma_m / D_m^{1/2} \quad (\text{A.18})$$

Courant and Hilberts resulting expression for λ_m is

$$\lambda_m = \frac{u_m - \sum_{n=0}^{m-1} (u_m \lambda_n) \lambda_n}{D_m^{1/2}} \quad m = 0, 1, \dots, \quad n = 0, 1, \dots \quad (\text{A.19})$$

where $D_m^{1/2}$ is given by,

$$D_m^{1/2} = (\gamma_m \gamma_m)^{1/2} \quad (\text{A.20})$$

From equation (A.18) and (A.19)

$$\lambda_m = u_m - \sum_{n=0}^{m-1} (u_n) (\lambda_n) \lambda_n \quad m = 0, 1, 2, \dots, \quad n = 0, 1, \dots \quad (\text{A.21})$$

$$\text{Now } \lambda_m = u_m - \sum_{n=0}^{m-1} (u_n \gamma_n) \gamma_n D_n^{-1} \quad (\text{A.22})$$

$$\text{also } D_m = (u_m u_m) - \sum_{n=0}^{m-1} (u_n \gamma_n)^2 D_n^{-1} \quad (\text{A.23})$$

$$\text{If } C_{mn} = (u_n \gamma_n) D_n^{-1} \quad (\text{A.24})$$

$$\text{Then } \gamma_m = u_m - \sum_{n=0}^{m-1} c_{mn} \gamma_n \quad (\text{A.25})$$

and equation (A.19) gives

$$\lambda_m = \frac{u_m - \sum_{n=0}^{m-1} c_{mn} \gamma_n}{D_m^{1/2}} \quad (\text{A.26})$$

$$\text{Now } D_m = u_m u_m - \sum_{n=0}^{m-1} c_{mn}^2 D_n \quad m = 0, 1, 2, \dots, \quad n = 0, 1, \dots \quad (\text{A.27})$$

A.2.1 Introduction of Constant J_{mn}

Assume the γ_m to be the linear function of u_0, u_1, \dots . Upon expanding the right side of equation (A.22) is given by

$$\gamma_m = u_m - \sum_{n=0}^{m-1} J_{mn} u_n \quad (\text{A.28})$$

where J_{mn} are the coefficients of the u_n in a given γ_m

Now deriving the recursion formula for J_{mn} by placing expression for γ_n in equation (A.25) gives

$$J_{mn} = c_{mn} - \sum_{r=n+1}^{m-1} c_{mr} J_{nr} \quad m = 2, 3, 4, \dots, \quad n = 1, 2, 3, \dots \quad (\text{A.29})$$

A.2.2 Formula for C_{mn}

To find an expression for C_{mn} , substitute the values of $\gamma_0, \gamma_1, \dots$ from equation (A.28) into (A.24). Then general formula is

$$c_{mn} = \frac{u_{mn} - \sum_{r=0}^{n-1} J_{nr} u_{nr}}{D_n} \quad m = 1, 2, 3, \dots, \quad n = 0, 1, 2, \dots, m-1 \quad (\text{A.30})$$

A.2.3 Formula for B_m

By considering equations (A.17) and (A.18)

$$B_m = \int_{\beta}^{\alpha} f(x) \gamma_m D^{-1/2} dx \quad (\text{A.31})$$

Now define the dimensionless constant E_m

$$E_m = B_m D_m^{-1/2} \quad \text{or} \quad B_m = E_m D_m^{1/2} \quad (\text{A.32})$$

From which it is found that

$$E_m D_m = \int_{\beta}^{\alpha} f(x) y_m dx \quad (\text{A.33})$$

Now we define the dimensionless constant G_m by

$$G_m = E_m D_m \quad (\text{A.34})$$

Now recursion formula for G_m

$$G_m = w_m - \sum_{n=0}^{m-1} c_{mn} G_n \quad m = 0, 1, 2, \dots \quad (\text{A.35})$$

recursion formula for E_m

$$E_m = \frac{w_m - \sum_{n=0}^{m-1} c_{mn} G_n}{D_m} \quad m = 0, 1, 2, \dots, \quad n = 0, 1, 2, \dots, m-1 \quad (\text{A.36})$$

Now recursion formula for B_m

$$B_m = \left[w_m - \sum_{n=0}^{m-1} c_{mn} D_n^{1/2} B_n \right] D_m^{-1/2} \quad (\text{A.37})$$

$$m = 0, 1, 2, \dots$$

$$n = 0, 1, 2, \dots$$

A.2.4 Formula for the A_{Nm}

By considering

$$f_N(x) = E_0 u_0 + E_1 (u_1 - J_{10} u_0) + E_2 (u_2 - J_{20} u_0 - J_{21} u_1) + \dots$$

$$f_2(x_0) = (E_0 - E_1 J_{10} - E_2 J_{20}) u_0 + (E_1 - E_2 J_{21}) u_1 + E_2 u_2 \quad (\text{A.38})$$

and from equation (A.14) for $N=2$,

$$f_2(x) = A_{20}u_0 + A_{21}u_1 + A_{22}u_2 \quad (\text{A.39})$$

Now comparing the above two equations

$$A_{20} = E_0 - E_1J_{10} - E_2J_{20}$$

$$A_{21} = E_1 - E_2J_{21}$$

$$A_{22} = E_2$$

Repeating the above procedure, A_{Nm} is obtained by many values of N and m . General formula for A_{Nm} is

$$A_{Nm} = E_m - \sum_{p=m+1}^N E_p J_{pm} \quad m = 0, 1, 2, \dots, N \quad (\text{A.40})$$

A.3 Calculation of Well Discharge

The well discharge q can be calculated by using the expression for the potential function Φ . The discharge per unit thickness of aquifer,

$$q = -K\Delta\Phi \int_0^{2\pi} \left(\frac{\partial\Phi}{\partial r} \right)_{r=r_w} r d\theta \quad r_w \rightarrow 0 \quad (\text{A.41})$$

Where K is the hydraulic conductivity, multiply the above equation by the thickness h . The total flow rate for the well is

$$q = -\frac{2\pi Kh A_{10} \Delta\Phi}{\ln\left(\frac{a}{r_w}\right)} \quad (\text{A.42})$$

APPENDIX B

CALCULATION OF ZONE TEMPERATURE DURING SOAK AND
PRODUCTION PERIOD (Tamim, 1995)

The hot and warm zone temperatures are calculated by making the following assumptions are: the vaporization effects are negligible and the thermal and fluid properties are essentially constant for a small time step. The energy balance for the hot and warm zone becomes,

$$-A_1 h M_1 \frac{dT_1}{dt} = q_1 \rho_1 C_{p1} - q_2 \rho_2 C_{p2} (T_1 - T_2) + (2A_1 + A_b) (\alpha_s T_1 - K \alpha_{21}), \quad (B.1)$$

$$-A_2 h M_2 \frac{dT_2}{dt} = q_2 \rho_2 C_{p2} (T_1 - T_2) + 2A_2 (\alpha_s T_2 - K \alpha_{22}) - A_t (\alpha_s T_1 - K \alpha_{21}). \quad (B.2)$$

Where T_1 and T_2 are the average hot and warm zone temperatures respectively. The hot and warm zone equations can be further expanded into

$$\frac{dT_1}{dt} = -\frac{q_1 \rho_1 C_{p1}}{A_1 h M_1} (T_1 - T_R) + \frac{q_2 \rho_2 C_{p2}}{A_1 h M_1} (T_1 - T_2) - \frac{\alpha_s (2A_1 + A_b)}{A_1 h M_1} + \frac{k_s \alpha_{21} (2A_1 + A_b)}{A_1 h M_1}$$

$$\frac{dT_1}{dt} = (\beta_2 - \beta_1 - \beta_3) T_1 + \beta_1 T_R - \beta_2 T_2 + \beta_4$$

$$\frac{dT_1}{dt} = \beta_5 T_1 - \beta_2 T_2 + \beta_6 \quad (B.3)$$

$$(D - \beta_5) T_1 + \beta_2 T_2 - \beta_6 = 0 \quad (B.4)$$

Similarly for warm zone,

$$\frac{dT_2}{dt} = (\beta_7 - \beta_8)T_2 - (\beta_7 - \beta_{11})T_1 + \beta_9 - \beta_{12}$$

$$\frac{dT_2}{dt} = \beta_{10}T_2 - \beta_{12}T_1 + \beta_{14} \quad (\text{B.5})$$

$$\beta_{13}T_1 + (D - \beta_{10})T_2 - \beta_{14} = 0 \quad (\text{B.6})$$

Now the following differential equation have been solved

$$(D - \beta_3)T_1 + \beta_2T_2 = \beta_6 \quad (\text{B.7})$$

$$\beta_{13}T_1 + (D - \beta_{10})T_2 = \beta_{14} \quad (\text{B.8})$$

Subject to the initial conditions, the two average temperatures can be expressed as

$$T_1 = C_1e^{\lambda_1 t} + C_2e^{\lambda_2 t} + \frac{P}{B}, \quad (\text{B.9})$$

$$T_2 = \frac{\beta_3 - \lambda_1}{\beta_2} C_1e^{\lambda_1 t} + \frac{\beta_3 - \lambda_2}{\beta_2} C_2e^{\lambda_2 t} + \frac{\beta_5 P}{\beta_2 B} + \frac{\beta_6}{\beta_2} \quad (\text{B.10})$$

where the following definitions have been employed

$$C_1 = \frac{\beta_2 T_2^0 - T_1^0 (\beta_3 - \lambda_2) - \beta_6 - \lambda_2 \frac{P}{B}}{\lambda_2 - \lambda_1} \quad (\text{B.11})$$

$$C_2 = T_1^0 - C_1 - \frac{P}{B} \quad (\text{B.12})$$

$$\beta_1 = \frac{q_1 \rho_1 C_{p1}}{A_1 h M_1} \quad (\text{B.13})$$

$$\beta_2 = \frac{q_2 \rho_2 C_{p2}}{A_2 h M_2} \quad (\text{B.14})$$

$$\beta_3 = \frac{\alpha_s (2A_1 + A_b)}{A_1 h M_1} \quad (\text{B.15})$$

$$\beta_4 = \frac{k_h \alpha_{21} (2A_1 + A_b)}{A_1 h M_1} \quad (\text{B.16})$$

$$\beta_5 = \beta_2 - \beta_1 - \beta_3 \quad (\text{B.17})$$

$$\beta_6 = \beta_1 T_R + \beta_4 \quad (\text{B.18})$$

$$\beta_7 = \frac{q_2 \rho_2 C_{p2}}{A_2 h M_2} \quad (\text{B.19})$$

$$\beta_8 = \frac{2\alpha_2}{h M_2} \quad (\text{B.20})$$

$$\beta_9 = \frac{2k_h \alpha_{22}}{h M_2} \quad (\text{B.21})$$

$$\beta_{10} = \beta_7 - \beta_8 \quad (\text{B.22})$$

$$\beta_{11} = \frac{A_b \alpha_2}{A_2 h M_2} \quad (\text{B.23})$$

$$\beta_{12} = \frac{A_b k_h \alpha_{21}}{A_2 h M_2} \quad (\text{B.24})$$

$$\beta_{13} = \beta_7 - \beta_{11} \quad (\text{B.25})$$

$$\beta_{14} = \beta_9 - \beta_{12} \quad (\text{B.26})$$

$$B = \beta_{13} \beta_2 - \beta_3 \beta_{10} \quad (\text{B.27})$$

$$P = \beta_6 \beta_{10} - \beta_2 \beta_{14} \quad (\text{B.28})$$

APPENDIX C

CALCULATION OF HEAT LOSS TO THE CAP AND BASE ROCK

(Tamim, 1995)

The heat loss to the cap and base rock were evaluated by using the approximation of Vinsome and Westerveld (1980). The equation of heat flow to the cap and base rock is

$$\frac{\partial T}{\partial t} = \alpha_h \frac{\partial^2 T}{\partial z^2}. \quad (C.1)$$

For the case of an interface condition,

$$\frac{\partial T_0}{\partial t} = \alpha_h \frac{\partial^2 T}{\partial z^2} \Big|_{z=0}. \quad (C.2)$$

The solution of the above equation gives the following expression for the cumulative heat stored in the cap rock and heat loss rate.

$$E_c = \frac{k_h}{\alpha_h} d (T_0 + Pd + 2qd^2) \quad (C.3)$$

$$\dot{q}_L = k_h \left(\frac{T_0}{d} - P \right) \quad (C.4)$$

where the following definitions were used,

$$P = \frac{\frac{\alpha_h T_0 \Delta t}{d} + T_0 - \frac{d^2 (T_0 - T_0^n)}{\alpha_h \Delta t}}{3d^2 + \alpha_h \Delta t} \quad (C.5)$$

$$q = \frac{2pd - T_0 + \frac{d^2 (T_0 - T_0^n)}{\alpha_h \Delta t}}{2d^2} \quad (C.6)$$

$$d = \frac{\sqrt{\alpha_h t}}{2} \quad (C.7)$$

$$I^n = T_0^n d^n + p^n (d^n)^2 + 2q^n (d^n)^3 \quad (\text{C.8})$$

Now the heat loss rate was expressed as

$$\dot{q}_L = \alpha_* T_0 - k \alpha_{n2} \quad (\text{C.9})$$

where $\alpha_* = k \left(\frac{1}{d} - \alpha_{n1} \right)$

$$\alpha_{n1} = \frac{\alpha_h \Delta t}{d(3d^2 + \alpha_h \Delta t)} - \frac{d^3}{\alpha_h \Delta t(3d^2 + \alpha_h \Delta t)} \quad (\text{C.10})$$

$$\alpha_{n2} = \frac{T_0^n}{\alpha_h \Delta t(3d^2 + \alpha_h \Delta t)} + \frac{I^n}{3d^2 + \alpha_h \Delta t} \quad (\text{C.11})$$

APPENDIX D

AVERAGE ZONE SATURATIONS (Tamim, 1995)

The average zone saturations were calculated on the basis of the following assumptions.

1. The saturation profiles in the hot and warm zone can be represented by an average zone values.
2. The time step for each cycle during production period is small compared with the total production time of the cycle.

The mobile oil and water saturations at any time $n+1$ in the hot and warm zones are given by the following expressions (Arthur et al., 1991).

$$S_{\text{omh,w}}^{n+1} = S_{\text{omh,w}}^n \exp^{-x_1(t^{n+1}-t^n)} + \frac{x_2}{x_1} \left(1 - \exp^{-x_1(t^{n+1}-t^n)} \right), \quad (\text{D.1})$$

$$S_{\text{wmh,w}}^{n+1} = S_{\text{wmh,w}}^n \exp^{-x_3(t^{n+1}-t^n)} + \frac{x_3}{x_1} \left(1 - \exp^{-x_3(t^{n+1}-t^n)} \right), \quad (\text{D.2})$$

where the following definitions are used,

For hot zone,

$$x_1 = \frac{-q_{o1} - q_{w1} + q_{o2} + q_{w2}}{V_{\text{hot}}}, \quad (\text{D.3})$$

$$x_2 = \frac{-q_{o1}\rho_{o1} + q_{o2}\rho_{o2}}{\rho_{o1}V_{\text{hot}}}, \quad (\text{D.4})$$

$$x_3 = \frac{-q_{w1}\rho_{w1} + q_{w2}\rho_{w2}}{\rho_{w1}V_{\text{hot}}}. \quad (\text{D.5})$$

For warm zone,

$$x_1 = \frac{q_{01} + q_{w1} - q_{02} - q_{w2}}{V_{warm}}, \quad (D.6)$$

$$x_2 = \frac{-q_{02}}{V_{warm}}, \quad (D.7)$$

$$x_3 = \frac{-q_{w2}}{V_{warm}}. \quad (D.8)$$

Now the following equations were used for calculating the saturation values,

$$S_{wh,w} = S_{wmh,w} + S_{wc} \quad (D.9)$$

$$S_{oh,w} = 1 - S_{wmh,w}. \quad (D.10)$$

APPENDIX E

CALCULATION OF PSEUDO-RELATIVE PERMEABILITIES

In CSS process the alteration of relative permeability is an important phenomena. The flow rate from shear failed zone of heavy oil reservoir mostly depends on the relative permeability of the reservoir fluids. Ito, Settari, and Jha (1993) presented an empirical formula for calculating pseudo-relative permeabilities of shear failed reservoir.

E.1 Multiplication Approach

Assuming that the k_w in fully failed zone is a product of a multiplier, X , and the reservoir relative permeability $k_{rw,res}$. Then the reservoir failed to a certain degree f , the pseudo-relative permeability is

$$k_{rw} = (1-f) \times k_{rw,res} + f \times X \times k_{rw,res} \quad (E.1)$$

$$k_{ro} = (1-f) \times k_{ro,res} + f \times X \times k_{ro,res} \quad (E.2)$$

E.2 Equations for Multiplication Factor

The multiplication factor depends on the failure pressure of the reservoir. Assuming the higher and lower pressure in the failure zone during production period are 1500 kPa and 300 kPa respectively. The extreme values of multiplication factor at that pressure are (Ito et al. 1993)

1. $P_{sh} = 1500$ kPa, $X_w = 20$ and $X_o = 0.2$
2. $P_{sh} = 300$ kPa, $X_w = 1.0$ and $X_o = 1.0$

Then the equations for multiplication factor can be defined by linearly interpolating between higher and lower pressure,

$$X_w = 3.25 \times 10^{-2} \times P_{\text{est}} - 8.750, \quad (\text{E.3})$$

$$X_o = -5.0 \times 10^{-4} \times P_{\text{est}} + 1.150. \quad (\text{E.4})$$

E.3 Equation for Degree of Failure

The degree of failure f can be defined by linearly interpolating in the failure zone between a higher and lower pressure range during production period. For higher pressure, $P_{\text{est}} = 1500$ kPa, the corresponding failure factor, $f = 0.14$ and for lower pressure $P_{\text{est}} = 300$ kPa, the failure factor, $f = 0.0$.

The equation for the degree of failure,

$$f = 1.667 \times 10^{-4} \times P_{\text{est}} - 0.035. \quad (\text{E.5})$$

Upon calculating the values of X and f , the corresponding values of pseudo-relative permeability are calculated for every time step during production period.

APPENDIX F

CALCULATION OF FLUID PROPERTIES

F.1 Calculation of Steam Properties

Steam is the heating agent for cyclic steam stimulation process. The calculations of steam properties are the essential part of CSS process. Steam tables are required for calculating various steam properties. For convenience of calculation, a set of polynomials (Tortike and Farouq Ali, 1989) were used for the present work. All the units are in SI metric.

F.1.1 Properties of steam Condensate

Calculation of Viscosity

The following equation was used for calculating the viscosity of steam condensate

$$\mu_{sc} = -0.0123274 + \frac{271038}{T} - \frac{235255}{T^2} + \frac{101425 \times 10^7}{T^3} - \frac{217342 \times 10^9}{T^4} \quad (\text{F.1})$$

273.15 ≤ T ≤ 645 K

Calculation of Density

$$\rho_{sc} = 378631 - 372487T + 0.196246T^2 - 5.0408 \times 10^{-4}T^3 + 6.29368 \times 10^{-7}T^4$$

273.15 ≤ T ≤ 645 K (F.2)

F.1.2 Properties of Steam Vapor

Calculation of Viscosity

$$\mu_{\text{g}} = -5.46807 \times 10^{-4} + 6.69490 \times 10^{-6} T - 3.3999 \times 10^{-8} T^2 + 8.29842 \times 10^{-11} T^3$$
$$273.15 \leq T \leq 645 \text{ K} \quad (\text{F.3})$$

Calculation of Density

$$\ln \rho_{\text{g}} = -93.7072 + 0.833941 T - 0.003208 T^2 + 6.57652 \times 10^{-6} T^3 - 6.92747 \times 10^{-9} T^4$$
$$273.15 \leq T \leq 645 \text{ K} \quad (\text{F.4})$$

F.1.3 Calculation of Latent Heat of Vaporization

$$L_{\text{v}} = \left(7184500 + 11048.6 T - 88.4050 T^2 + 0.162561 T^3 - 1.21377 \times 10^{-4} T^4 \right)^{1/2}$$
$$273.15 \leq T \leq 645 \text{ K} \quad (\text{F.5})$$

F.1.4 Calculation of Saturation Temperature

$$T_{\text{s}} = 280.034 + 14.0856 \ln p + 13807 (\ln p)^2 - 0.101806 (\ln p)^3 + 0.019017 (\ln p)^4$$
$$.611 \text{ kPa} \leq p \leq 22.12 \text{ Mpa} \quad (\text{F.6})$$

F.1.5 Calculation of Saturation Pressure

$$P_s = \left(-175.776 + 2.292727T - 0.011395T^2 + 2.6278 \times 10^{-5}T^3 - 2.73726 \times 10^{-8}T^4 \right)^2$$

$80 \leq T \leq 647.3 \text{ K} \quad (\text{F.7})$

F.2 Calculation of Oil Properties

F.2.1 Calculation of Viscosity

The flow rate into the well bore depends on the viscosity values of the reservoir oil. Farouq Ali (1982) presented a good approximate method in terms of dynamic viscosity for calculating oil viscosity.

$$\mu_o = ae^{b/(T+273.15)} \quad (\text{F.8})$$

where $a = 6.54053 \text{ E-15}$ for $T \leq 373.15 \text{ K}$

$$b = 11380.31$$

and

$$a = 1.77632 \text{ E-7,} \quad \text{for } T > 373.15 \text{ K}$$

$$b = 4993.018$$

F.2.2 Calculation of Density

The following correlation was used to calculate the oil density by using a thermal expansion factor,

$$\rho_o = \rho_{oR} \{ 1 - \beta_o (T - T_{oR}) \} \quad (\text{F.9})$$

Where the subscript R represents standard condition.

F.2.3 Calculation of Specific Heat

Smith-Magowan et al. (1982) presented the following equation for calculating the oil sand specific heat,

$$C_p = 1557 + 5.219 \times 10^{-3}T - 8.686 \times 10^{-6}T^2. \quad (\text{F.10})$$

